



# Journal of Electronic Systems and Programming

Journal of Electronic Systems and Programming

Issue N0:5 June 2022

Issue N0:5 June 2022

**Journal of Electronic Systems and Programming**

**Electronic Systems and Programming Center**

**Journal  
of  
Electronic Systems  
and Programming**

**Issue No: 5 - 2022**

| <b>Editorial Board</b>         |                 |
|--------------------------------|-----------------|
| Mr. Abadul Hakim Alhadi Anaiba | Journal Manager |
| Dr. El-Bahlul Fgee             | Editor-in-Chief |
| Dr. Khari A. Armih             | Member          |
| Dr. Mustafa Kh. Aswad          | Member          |
| Dr. Moktar M. Lahrashe         | Member          |
| Dr. Abdusamea omer             | Member          |

**Editorial:**  
**5<sup>th</sup> Issue – Journal of Electronic Systems and Programming**

We are delighted to announce the publication of the 5<sup>th</sup> issue of the Journal of Electronic Systems and Programming (JESP).

First of all, we would like to express our gratitude to the all members of Electronic Systems and Programming Center for their unlimited support and dedication that has made JESP what it is today.

As the official publication of Electronic Systems and Programming Center (EPC), the JESP continues to provide a platform for both researchers from inside and outside the center to share their novel results and latest developments, and also to seek better understanding of the current situation on research related to the area of contributions of EPC.


Finally, we thank our editorial board team, reviewers and authors for their fundamental contribution to the third release of the Journal. We still hope authors could consider JESP to be the best place where to publish their work.

Editorial Board

**Table of Contents:**

|          |   |                |
|----------|---|----------------|
| <b>1</b> | <b>Prediction of friction coefficient of pin-on-disc test using artificial neural network</b>         | <b>1-22</b>    |
| <b>2</b> | <b>Authentication and Verification Of E-Certificates Using Watermarking and Encryption Techniques</b> | <b>23-38</b>   |
| <b>3</b> | <b>Public Health and ELF Fields<br/>Case Study</b>  | <b>39-54</b>   |
| <b>4</b> | <b>Effect of Dust Storm on WiMAX System in Libyan Desert Environment</b>                              | <b>55-70</b>   |
| <b>5</b> | <b>Optimizing Submerged ARC Welding Process Variables Using Taguchi Method</b>                        | <b>71-92</b>   |
| <b>6</b> | <b>Behavioral Intention of Youth Using Facebook in Learning in Libya (Bani Waleed as Model)</b>       | <b>93--111</b> |





**PREDICTION OF FRICTION COEFFICIENT  
OF PIN-ON-DISC TEST USING ARTIFICIAL  
NEURAL NETWORK**

**1**





## Prediction of friction coefficient of pin-on-disc test using artificial neural network

A.Shebani  
College of Computer Technology Zawia  
[amershebani@gmail.com](mailto:amershebani@gmail.com)

### Abstract

Understanding the nature of wear in the railway field is of fundamental importance to the safe and cost effective operation of the railways. Accurate prediction of this wear can improve economy, ride comfort, prevention of derailment and planning of maintenance interventions. Poor prediction can result in failure and consequent delay and increased costs if it is not controlled in an effective way. Pin on disc wear testing is used extensively for studying wear. The aim of this paper is to predict friction coefficient of pin on disc test using an artificial neural network. Experimental dataset of pin on disc test at different applied loads, and sliding distances with different time of test were used to train, and test the artificial neural networks (ANN). Results obtained from the developed radial basis function neural network (RBFNN) model were compared with measured results; it is found that the predicted and measured results showed good accuracy when the developed ANN model was trained with least mean square algorithm (LMS). Pin-on-disc test conducted, and then, the Alicona profilometer was used to measure the friction coefficient. Radial basis function neural network was developed to predict the friction coefficient of pin on disc test. The results demonstrate that the neural network can be used efficiently to predict friction coefficient of pin on disc test.

**Keywords:** friction coefficient prediction, artificial neural network, radial basis function neural network, Alicona profilometer.

## 1. Introduction

Wear coefficient, and friction coefficient are two of the key parameters in the performance of any two tribo-systems. Friction is defined as the resistance to relative motion between two bodies of contact. There are various types of friction, which include static, rolling, kinetic and fluid friction. Wear can be defined as the removal of material from solid surfaces by mechanical action. Wear of materials is an everyday experience and has been observed and studied for a very long time. A national survey indicated that the cost of wear to the UK industry was £650 million per year in 1997. Furthermore, the costs were about 0.25 percent of turnover for the companies who have wear problems. Generally, these costs can be reduced by making optimum design of the wheel/rail interface to eliminate or reduce the wear. Also, notable is the Hatfield accident in 2000 in Britain, which injured 34 people, killed 4 people, and led to the cost of £733 million in maintenance and compensation payments. In 1977, the Granville train disaster injured 213 and killed 83 people in Australia. These accidents were related to rolling contact fatigue (RCF), poor maintenance and wear. The friction coefficient is the ratio of the frictional resisting the motion of two surfaces in contact to the normal force pressing the two surfaces together. Mathematically, the friction coefficient =  $F/N$ , where  $F$  is the frictional force and  $N$  is the normal load [1], [2].

### 1.1 Types of Wear

There are many types of wear, but the main classification of wear and the specific wear mechanisms that occur in each type are shown in Figure (1) [3].

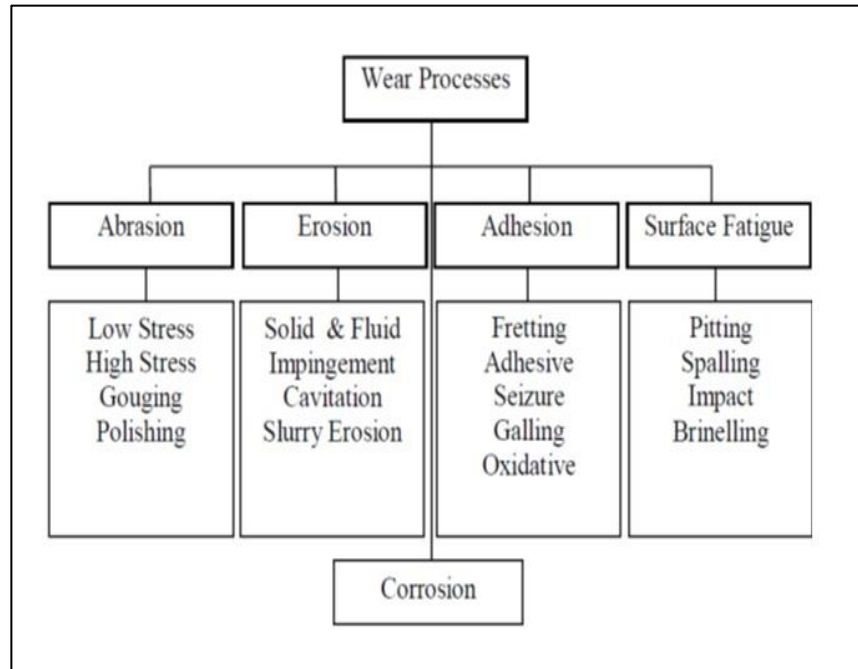


**Figure 1: Flow chart of various wear mechanisms [3].**

### 1.1.1 Adhesive Wear

Adhesive wear is classified as the fundamental type of wear. It occurs when two solid surfaces are in rubbing contact. When two surfaces are brought into contact, asperities of the two surfaces make physical contact.

The contact area between the two surfaces is localized to the small regions known as asperities, these asperities are referred to as junctions, see Figure (2) [4].

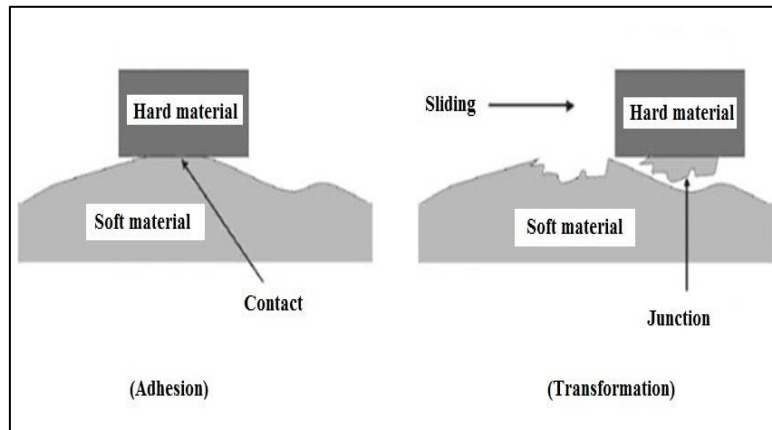


**Figure 2: Adhesive wear behaviour [4].**

### 1.1.2 Abrasive Wear

Abrasive wear occurs when a rough, hard surface slides on a softer surface. It occurs under two conditions. The first condition is the two body abrasion; where one surface is harder than the other rubbing surface, as shown in Figure 3. The second condition is the three body abrasion; in this case a small particle of grit lodges between the two softer rubbing surfaces as shown in Figure 3 [3].

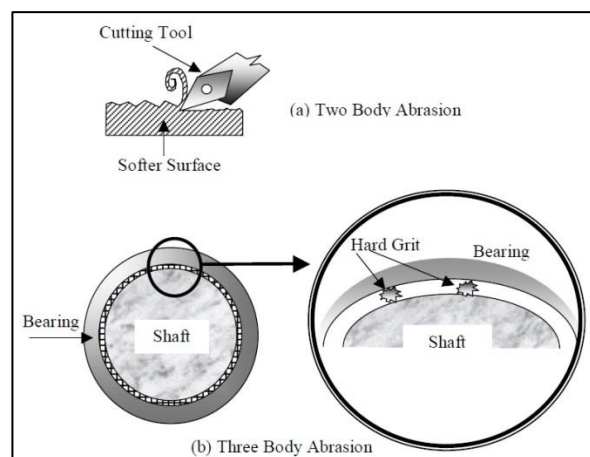


**Figure 3 Abrasive wear phenomena [3].**

### 1.1.3 Fatigue Wear

Fatigue wear occurs when a material yields to cyclic loading; it can be observed in rolling wear, sliding wear, and impacting wear processes as well. As the plastic strain accumulates, the movement of dislocations leads to the formation of microcracks below the surface; see Figure (4). Cracks are initially produced on the weak, imperfect, or otherwise damaged regions of the contact surface. These cracks grow and propagate through the surface of the material to form cracks under repeated sliding motion. When one surface continues to slide against another surface, the material on the contact surface is broken and wear debris is generated [5].

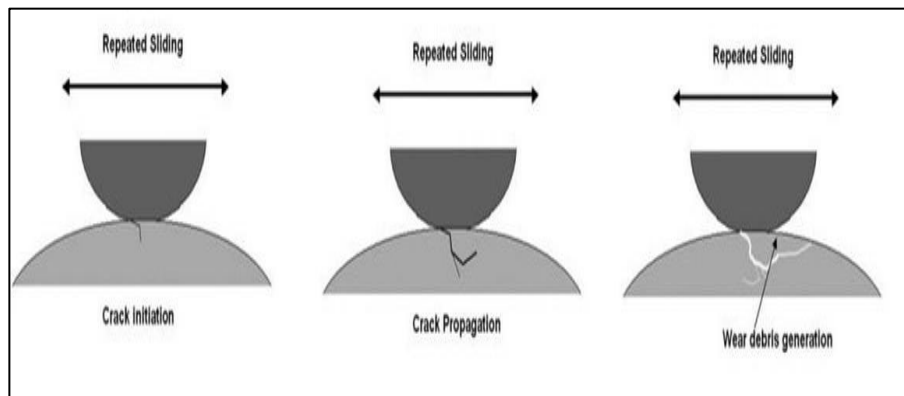


**Figure 4: Fatigue wear [5].**

### 1.1.4 Corrosion Wear

Corrosion wear is the deterioration of a material through chemical or electrochemical interaction with the environment. Electrochemical corrosion is defined as the chemical reaction accompanied by the passage of an electric current. Chemical corrosion occurs in high humidity and high temperature environments [6].

### 1.1.5 Erosion Wear

The erosion wear phenomenon is shown in Figure (5). When the solid particle A is impacted with solid surface B, a part of the surface B is removed. Several environmental parameters are associated with the erosion process, such as: impact velocity, impact angle, and particle size [7].

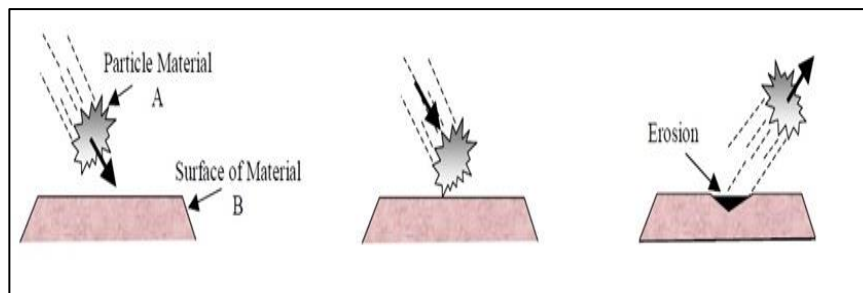


**Figure 5 Schematic of erosion wear [3].**

### 1.2 Roughness Parameters:

The definition of the most important roughness parameters are [8],[9]:

1. The Centre line average value ( $R_a$ ) or arithmetic average roughness; the arithmetic average value of filtered roughness profile determined from deviations about the center line within the evaluation length; the most popular parameter for a machining process and product quality control. This parameter is easy to define, easy to measure and gives a general description of surface amplitude. Though it lacks physical significance, it is established in almost every national standard for measuring roughness. On the other hand, it is insensitive to small variations in the profile and gives no information on the

in length characteristics, and also, it makes no distinction between peaks and valleys.

2. Maximum vertical distance ( $R_t$ ) or maximum peak to valley, the maximum peak to valley height of the filtered profile over the evaluation length is very sensitive to large deviations from the mean line and scratches; it is very commonly used along with  $R_a$  as a general indicator.
3. Root mean square roughness ( $R_q$ ), or RMS roughness; the root mean square average of the roughness profile ordinates; it is more sensitive to peaks and valleys than  $R_a$ .
4. Skewness of roughness ( $R_{sk}$ ), evaluates the degree of asymmetry in cases of asymmetric distribution and is characterized as positive or negative.
5. Kurtosis of roughness ( $R_{ku}$ ), describes the distribution sharpness and takes the value 3 for the normal distribution. For  $\xi > 3$  the surface is dominated by sharp peaks (spiky), whereas if the  $\xi < 3$  then the peaks are bumpy, where ( $R_{ku} = \xi$ ).

The centre line average value  $R_a$  is one of the most important roughness parameters; it is used to monitor a production process where gradual changes in the surface occur due to the wear. An instrument for measuring the centre line average value  $R_a$  should have a higher measuring repeatability. The definition of roughness  $R_a$  is shown in Figure (6):

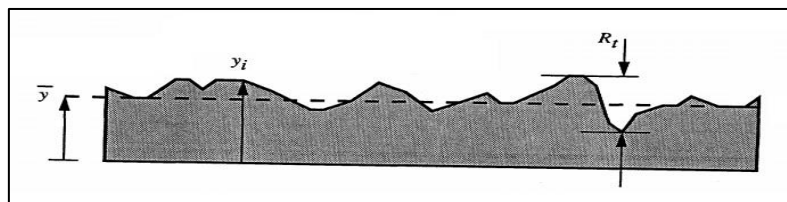


**Figure 6 Definition of average roughness parameter [8]**

The centre line average value ( $R_a$ ) also called the roughness average, Figure (4-5) shows the quantity  $R_a$  is the average deviation of the profile from mean line.

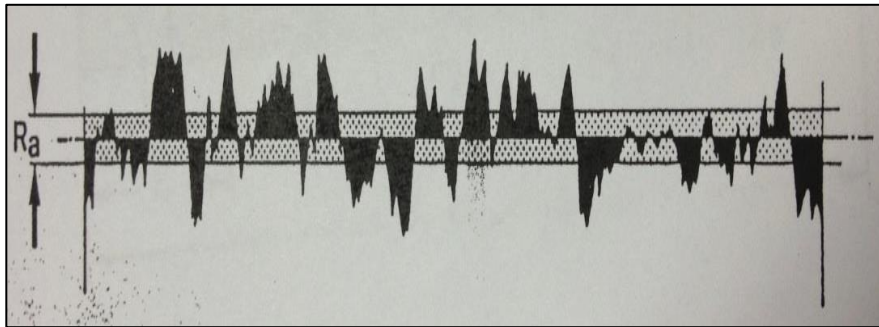


Figure 7 Quantity of average roughness parameter [9]

### 1.3 3D Surface Measurements

Figure (8) shows the 3D contact analysis of pin-on-disc, where  $F$  the normal is load, and  $R$  is the pin radius.

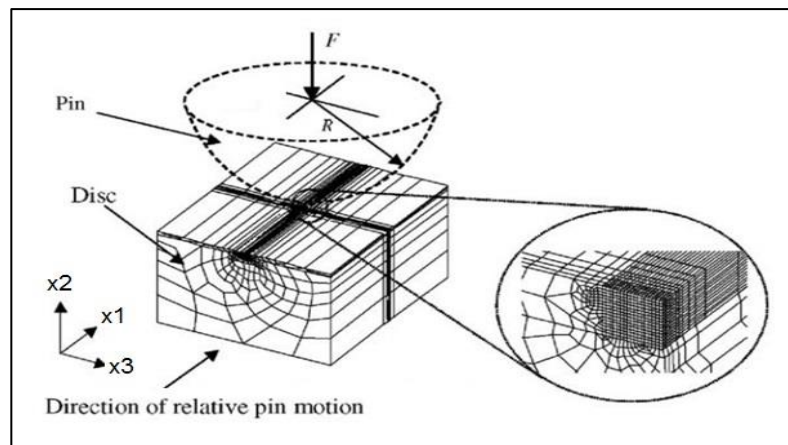


Figure 8 3D pin/disc contact analysis [10]



A 3D static contact analysis is important to study the wear behaviour. In Figure (4-10), the normal load is applied through the axis of the rigid pin head of the radius ( $R$ ) and the friction force exerted on the disc due to sliding is realized by applying a moment to the pin about the ( $x_3$ ) axis. Thus, the shear force in the static analysis acts along the direction of the motion of the pin relative to the disc in the actual sliding contact problem, i.e. along the ( $x_1$ ) direction.

## **2. Introductions to Artificial Neural Network (ANN)**

An artificial neural network can be categorised as a computational model which has the ability to learn. The neural networks are divided in terms of their structure into two types: feedforward network and recurrent network. In feedforward neural networks the information flows in one direction without feedback (loops). The information travelled from the inputs to the outputs and without feedback between output layer and input layer. The feedforward neural network can consists of more than one hidden layer. In recurrent neural network the information can a flow in forward direction and a backward direction (it contain feedback connections), the outputs of neurons can feedback to the same neurons or to neurons in previous layers [11]-[14].

### **2.1 Radial basis function neural network (RBFNN)**

A radial basis function neural network (RBFN) has an input, hidden, and output layer such as in Figure (9). The hidden layer consists of RBF activation function. Its training procedure is usually divided into two stages: The first stage includes selection of the centres and widths of the hidden layer; and the second stage is the weights adjustment. The centres of the radial basis function can be selected by using different strategies, but the common approaches are fixed centres selected at random, and K-Means clustering algorithm. One simple procedure for selecting the basis function centres  $C_i$  is to set them equal to a random subset of the input vectors from the training set, this

algorithm is called centre selection using a subset of data points [15]-[19].

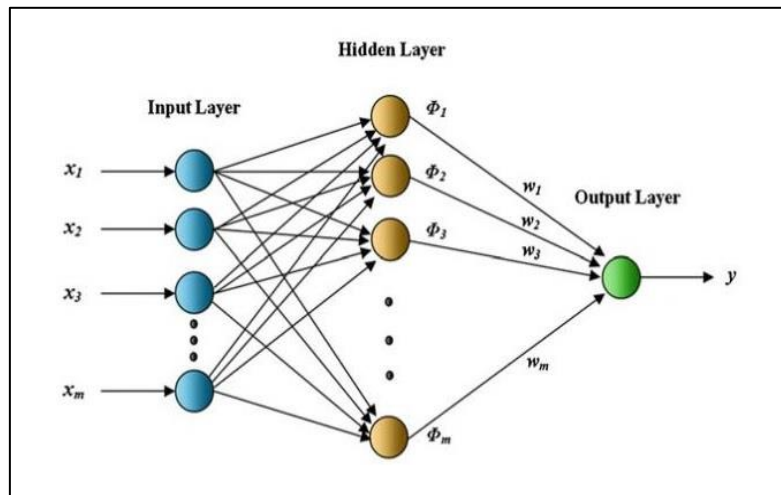


**Figure 9: Radial Basis Function Network Architecture [19]**

In  $X_1, X_2, X_3 \dots, X_m$  are inputs which are fed into the input layer. Computational units are in the hidden layer, which are called centres represented by  $C_1, C_2, \dots, C_m$ . Here, the dimension of each centre for  $m$  input network is  $m \times 1$ .

The output of RBFNN is [19]:

$$y = \sum_{j=1}^m W_j \phi_j \quad (1)$$

Where  $\phi$  is the activation function, and  $W$  is the weights.

The common activation functions  $\phi$  of RBFNN are [19]:

1. The inverse multiquadratic function:

$$\phi(x) = (r^2 - \sigma^2)^{-1/2} \quad (2)$$

2. The Gaussian function is:

$$\phi(x) = \exp\left(-\frac{r^2}{2\sigma^2}\right) \quad (3)$$

$$r = \|x - c\| \quad (4)$$

Where  $C$  is the centres,  $x$  is the inputs, and  $\sigma$  is the width of activation function.

There are many algorithms to select the centres such as Kohonen algorithm, K-means algorithm, and random selection of the centres. The K-Means clustering algorithm for selecting the centres of RBFNN such as in the following steps [20]:

1. From data set select random  $k$  points as initial cluster centres.
2. Calculate the distance of each sample to the cluster centres.
3. Recalculate the cluster centre according to the clustering result.
4. Re-cluster all the elements of the data set according to the new centre.
5. Repeat Step 4 until the clustering does not change.
6. Output the result.

Euclidean distance method is the most common method which can be used to calculate the width of activation function for RBFN such as in the following equation [20]:

$$dist = \sqrt{\sum_{i=1}^n (X_i - c_i)^2}, i = 1, 2, 3, \dots, n. \quad (5)$$

Where:  $X_i$  are the inputs,  $c_i$  are the centers, and  $n$  is the vector dimension.

The least mean square algorithm (LMS) is the most common algorithm which can be used for adapting the weights of the output layer for the RBFNN such as in the following steps [20]:

- i. Initialization of the weight vector.

$$W(t) = 0 \quad (6)$$

- ii. Calculate the network output for time steps.

$$W(t + 1) = W(t) + \mu e(t) \Phi^T(t) \quad (7)$$

$$e(t) = y(y) - y_m(t) \quad (8)$$

$$W(t + 1) = W(t) + \mu (y(t) - y_m(t)) \Phi^T(t) \quad (9)$$

Where  $W(t + 1)$  is the updated weights,  $W(t)$  is the previous weights originally set to zero,  $y(t)$  is the desired output,  $y_m(t)$  is the output of the network, and  $\Phi^T(t)$  is the hidden output (Gaussian output).

The learning factor  $\mu$  is ( $0 < \mu \leq 1$ ), it is a positive gain factor term that controls the adaptation rate of the algorithm,  $y$  and  $y_d$  are the actual output and the desired output respectively, and  $t$  is the current time.

The mean squared error is used for measuring the performance of the network, it can be written such as in the following equation [21]:

$$MSE = \sum_{i=1}^n \frac{(y_i - \tilde{y}_i)^2}{n} \quad (10)$$

Where  $y_i$  is the actual output and  $\tilde{y}_i$  is the estimated output.

### 3. Pin-on-disc test

#### 3.1 Experimental setup

The pin-on-disc (AEROTECH UNIDEX 11) is used in this project for the investigation of the effects of normal load and hardness of material on the wear under dry and sliding conditions.

In the pin-on-disc rig, two specimens were used; one, a pin with a tip, is positioned perpendicular to the disc. The pin upper specimen is perpendicular to the lower specimen which is a disc shown in Figure (10).

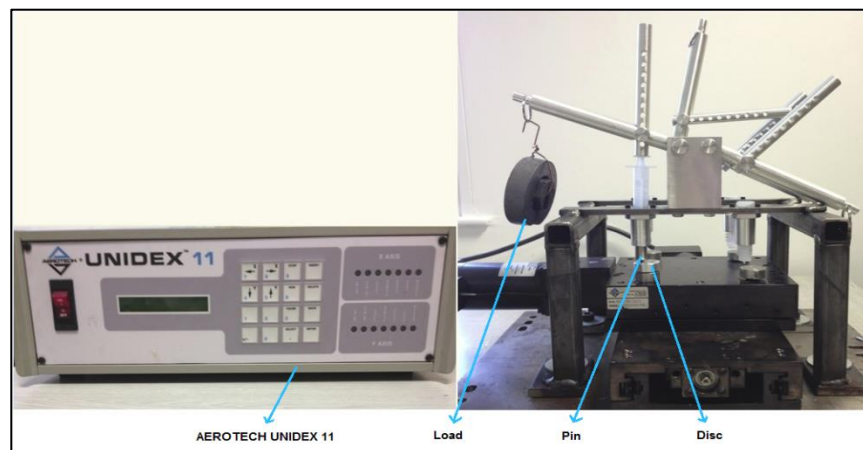


**Figure 10: Pin-on-disc (AEROTECH UNIDEX 11)**

Experiments were conducted at normal load varied from 4N to 10N, with test time of one 10 minute for each test; the sliding speed was 400mm/min, 500mm/min, and 600mm/min; while the sliding distance was 5mm. The materials which were used in the test were, disc made of aluminium 6082 and pin made of mild carbon steel EN8. The dimensions of the pin and disc were measured by using a micrometre, the pin dimensions were 49.49mm height and 11.98mm diameter; and the disc dimensions were 25.73mm in diameter and 9.08mm.

The wear test was conducted using the following steps:

1. Proper mass was added to the system lever in pin-on-disc tester.
2. The motor started and the speed is adjusted to the desired value while holding the pin specimen out of contact with the disk; and then the motor was stopped.
3. The pin and disc were inserted into their holders.
4. The timer was adjusted to the desired time (one hour).
5. The test was started with the specimens in contact under load.
6. After one hour the test was stopped (when the desired time was achieved).
7. The pin and disc were removed, to commence in wear measurements.

The next step for pin-on-disc test is to measure the friction coefficient of pin on disc test by using the Alicona (INFINITE FOCUS) which is shown in Figure (11).

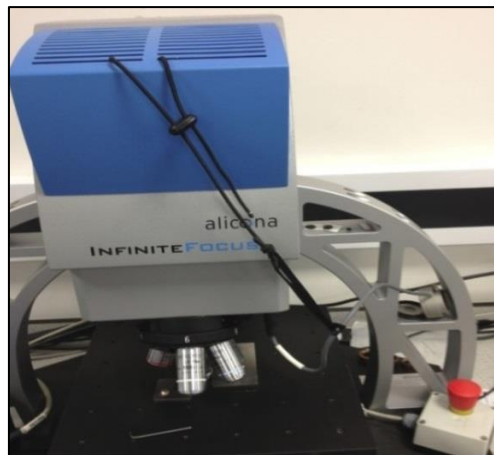


**Figure 11: Alicona (INFINITE FOCUS)**

#### 4. Artificial neural network model to predict the friction coefficient of pin-on-disc test

Figure 12 shows the artificial neural network model used to predict the friction coefficient of pin-on-disc test

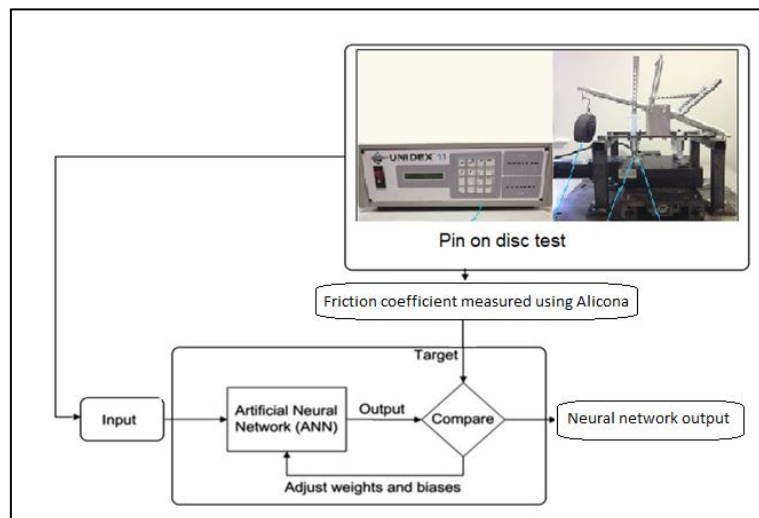
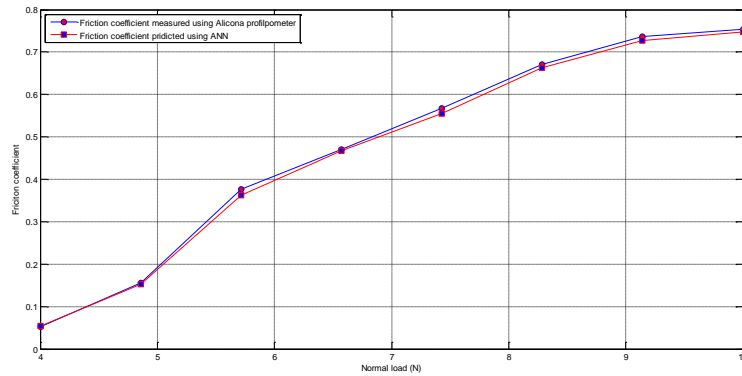


Figure 12: ANN model to predict the friction coefficient of pin/on disc test

#### 5. Results and Discussion

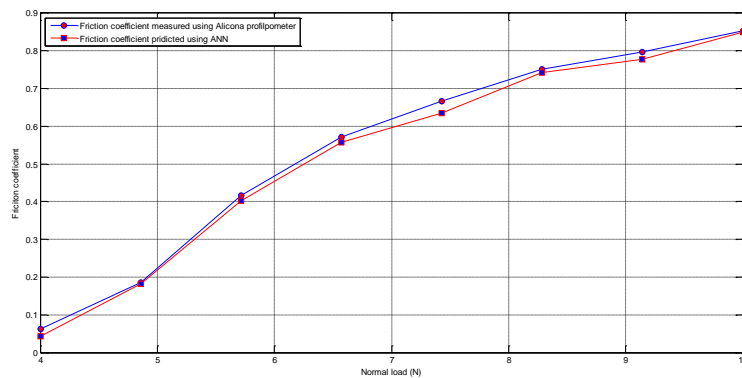
This section contains comparison between the friction coefficient measured using pin-on-disc tests, and friction coefficient predicted using artificial neural network.

Figure 13 shows the friction coefficient measured using Alicona profilometer and predicted using RBFNN (sliding speed of 400mm/min, while the normal load varied from 4N to 10N).



**Figure 13: Friction coefficient measured using Alicona profilometer and predicted using ANN (sliding speed of 400mm/min)**

Figure 14 shows the friction coefficient measured using Alicona profilometer and predicted using RBFNN (sliding speed of 500mm/min, while the normal load varied from 4N to 10N).



**Figure 14: Friction coefficient measured using Alicona profilometer and predicted using ANN (sliding speed of 500mm/min)**



Figure 15 shows the friction coefficient measured using Alicona profilometer and predicted using RBFNN (sliding speed of 600mm/min, while the normal load varied from 4N to 10N).

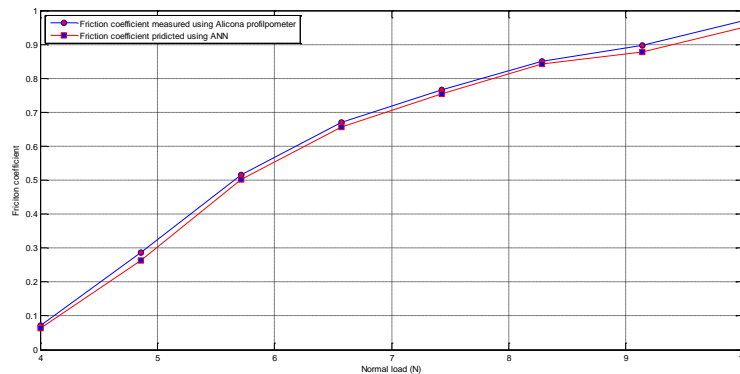


**Figure 15: Friction coefficient measured using Alicona profilometer and predicted using ANN (sliding speed of 600mm/min)**

Figure 13 shows that the friction coefficient increases from 0.054 to 0.751 with increasing of normal load, where sliding speed was 400mm/min, while the normal load varied from 4N to 10N.

Figure 14 shows that the friction coefficient increases from 0.062 to 0.854 with increasing of normal load, where sliding speed was 500mm/min, while the normal load varied from 4N to 10N.

Figure 15 shows that the friction coefficient increases from 0.073 to 0.956 with increasing of normal load, where sliding speed was 600mm/min, while the normal load varied from 4N to 10N.

This work focus on effect of normal load on friction coefficient, results show that the friction coefficient increases linearly with increase of normal load.

The main aim of this work was predict the friction coefficient using artificial neural network. Simulation results provided on Figure 13, Figure 14, and Figure 15 show that the mse was equal 4% on overall, which mean the accuracy of neural network model was 96%. The

mean squared error (mse) used for measuring the performance of the neural network. It can therefore be concluded that the RBFNN is an accurate models for friction coefficient prediction.

## **6. Conclusions**

In this paper, a radial basis function neural network was developed to predict the friction coefficient of pin-on-disc test subjected to different applied normal loads, and sliding speed. Tests result shows that the friction coefficient increased linearly with increase of normal load, and sliding speed. Experimental dataset at different applied loads, sliding speed, test time, and sliding distances were used as inputs to train, and test the artificial neural network (ANN); where the output of the neural network was the friction coefficient. Simulation results obtained from the developed radial basis function neural network (RBFNN) model were compared with experimental results, it is found that the experimental and measured results showed good accuracy when the developed ANN model was trained with least mean square algorithm (LMS). This paper also demonstrated the neural network as powerful tool for friction coefficient of pin-on-disc test prediction.

## References

- [1] M. J. Neale, and M. Gee, "Guide to Wear Problems and Testing for Industry", William Andrew Publishing, USA, 2001.
- [2] V. Reddy, "Development of an integrated model for assessment of operational risks in rail track", PhD thesis, Queensland University of Technology, School of Engineering Systems, Australia, 2007.
- [3] J. Stokes, "Theory and Application of the High Velocity Oxy-Fuel (HVOF) Thermal Spray Process", PhD thesis, School of Mechanical and Manufacturing Engineering, Dublin City University, Ireland, 2008.
- [4] B. Bhushan, "Tribology: Friction, Wear, and Lubrication", CRC Press LCC, USA, 2000.
- [5] R. Narayan, "Biomedical Materials", Springer, USA, 2009.
- [6] J. A. Collins, "Mechanical Design of Machine Elements and Machines", John Wiley & Sons, USA, 2002.
- [7] G. W. Stachowiak, "Wear: Materials, Mechanisms and Practice", John Wiley & Sons, UK, 2005.
- [8] P. J. Blau, R. L. Martin, and L. Riester, "A comparison of several surface finish measurement methods as applied to ground ceramic and metal surfaces", *Oak Ridge National Laboratory (Ornl)*, USA, 1996.
- [9] L. Mummery, "Surface Texture Analysis the Handbook", Hommlwerke GmbH, Germany, 1990.
- [10] W. Yan, N. P. Dowd, E. Busso, "Numerical study of sliding wear caused by a loaded pin on a rotating disc", *Journal of the Mechanics and Physics of Solids*, vol. 50, pp. 449 – 470, 2002. Elsevier Science Publishing, USA, 2002.
- [11] B. Kröse, B. Krose, P. van der Smagt, and P. Smagt, "An introduction to neural networks," 1993.

- [12] A. Zalzal and X. Liu, "Neural Networks for Identification, Prediction and Control," ed: Great Britain: Springer-Verlag London Limited, 1995.
- [13] C. R. Tosh and G. D. Ruxton, *Modelling perception with artificial neural networks*: Cambridge University Press, 2010.
- [14] G. Mihalakakou, M. Santamouris, and D. Asimakopoulos, "Modeling ambient air temperature time series using neural networks," *Journal of Geophysical Research: Atmospheres (1984–2012)*, vol. 103, pp. 19509-19517, 1998.
- [15] A. Fathy and A. Megahed, "Prediction of abrasive wear rate of in situ Cu–Al<sub>2</sub>O<sub>3</sub> nanocomposite using artificial neural networks", *The International Journal of Advanced Manufacturing Technology*, vol. 62, pp. 953-963, 2012.
- [16] H. H. W. Yu, and N. Zhang, "Advances in Neural Networks", Springer Publishing, China, 2009.
- [17] S. Haykin and N. Network, "Neural Networks: A comprehensive foundation", vol. 2, 2004.
- [18] R. J. Howlett and L. C. Jain, "Radial basis function networks 2: New Advances in Design", vol. 67: Springer Science & Business Publishing, 2001.
- [19] M. K. Kundu, "Advanced Computing, Networking and Informatics", Springer Publishing, Switzerland, 2014.
- [20] G. M. Fathalla, "Analysis and implementation of radial basis function neural network for controlling non-linear dynamic systems", PhD thesis, Faculty of Engineering University of Newcastle, UK, 1998.
- [21] L. D. Fredendall and E. Hill, "Basics of supply chain management", CRC Press, 2000.



**Authentication and Verification Of  
E-Certificates Using Watermarking and  
Encryption Techniques**

**2**



## Authentication and Verification Of E-Certificates Using Watermarking and Encryption Techniques

Mohamed Ab. Sultan

Department of Electrical and Electronics Engineering  
Higher Institute of Science and Technology Zawia, Libya  
[abo\\_sultan2020@yahoo.com](mailto:abo_sultan2020@yahoo.com)

Nuha Omran Abokhdair

Computer Science Department, Faculty of Science  
University of Zawia, Zawia, Libya  
[abo.khdeir@zu.edu](mailto:abo.khdeir@zu.edu)

Rawad Masoud Salim Salman

Computer Science Department, Faculty of Science  
University of Zawia, Zawia, Libya  
[Rawadsalman@zu.edu.ly](mailto:Rawadsalman@zu.edu.ly)

Haitham S. Ben Abdelmula

College of Computer Technology Zawia, Libya  
[hsaa8383@gmail.com](mailto:hsaa8383@gmail.com)

### **Abstract**

Nowadays forging degree certificates is extremely easy and inexpensive. This makes the process of certificate validation and authentication complicated. The proposed model in this paper is used to validate and authenticate certificates by issuing an electronic certificate which is watermarked by the issuer university logo. The logo is encrypted and the encryption key is also encrypted using the private key of the issuer university. The encrypted key is converted to a barcode and appended to the e-certificate in order to authenticate the source of certificate. The process of watermarking will ensure the integrity of the certificate. This model does not use any network-

dependent processes, which makes it an off-line and secure process that helps maintaining users' information privacy.

**Keywords:** Authentication - e-certificate - cryptography - watermarking - barcode.

## 1. Introduction

In most countries, universities and institutions issue paper-based certificates to graduated students to ensure that they have successfully completed requirements of their study. These certificates can easily be lost or damaged. Therefore, reissuing the certificate requires a fairly complicated procedure. Moreover, counterfeit paper-based certificates becomes very popular and demanded with the advance of copying and printing technologies which are easily available at cheaper costs [1-3]. In the current situation, to verify the authenticity of the degree certificate, the verifier has to contact the certificate issuer. This process is costly and time consuming since it involves multiple level of human interaction [2].

On the other hand, since the outbreak of coronavirus pandemic the education sector is following e-learning or online mode to conduct classes. Furthermore, most of job applications and postgraduate applications require certificate's holder to submit a softcopy of the certificate.

Therefore, this research encourages universities and educational institutions to issue an electronic form of certificates (e-certificate) beside the paper form in order to solve issues related to paper certificate management and for its portability [2]. In addition, it proposes a verification model for the issued e-certificate. This e-certificate will be watermarked with the encrypted logo of the issuer in order to verify and authenticate it by the viewer.



## 2. Related Work

As the number of discovered fake certificates is raised, there are many recent researches proposed techniques to authenticate and verify certificates in paper form or in electronic form.

Researchers in [4] proposed a prototype for authenticating of secondary school certificates in Kenya using QR code and digital signature. This prototype is a web-based prototype. It generates the QR after hashing the certificate details and signing the hash using the issuer private key. The generated QR is attached to the certificate. During the verification process, the viewer will scan the QR code to generate the QR code validation key which will be entered to the system portal and open it if the certificate id valid.

Another model called Robust Visible Digital Stamp RVDS is introduced in [5]. In this model the document information is compressed and encrypted. The encrypted data is hashed and signed. The QR is created by including the encrypted data and the digital signature. The process of verification starts with first verifying the digital signature and second decrypting the encrypted data. A combination of pre-shared key, machine signature, and time stamp is embedded into the QR code in masked forms in addition to the encrypted data and the signature. This combination is extracted and unmasked to be used as key for the decryption process. This mechanism leads to key distribution issue.

In [6], two phases of document authentication are presented. The first is the document creation, where the text content of the document is hashed and signed. The hash value and the signature are compressed and encoded in QR code, which will be printed on the document. The second phase is verification phase, where the received document is scanned and the text of the document is extracted using OCR software. This text will be hashed and compared to the hash extracted from the QR code. Nevertheless, OCR technique is not accurate and require human interaction to ensure its accuracy .

Researchers in [7] proposed a watermarking technique to authenticate digital documents. It uses biometric data collected from the Indian citizen to generate biometric watermarked document to identify the owner of the document using a secret key. This technique is able to position the modified blocks. However, using the same secret key in issuing and verifying the document will cause an issue of key exchanging. Moreover, the authenticating process require retrieving the biometric code from the database

Chen-wilson and Argles designed a system to secure e-certificates [8]. In this system, educational institution will issue a digitally signed, time stamped and encrypted e-certificate and send it to the student through a secured emailing system. The student is able to view and set new access controls to the received e-certificate using the proposed system before sending it to the reviewers. The reviewers are able to use the control system to verify the access-controlled e-certificate.

Finandhita and Afrianto introduced an electronic diploma model based on digital signature [9]. Four users are involved in this web-based system including: system operators, head of the university, alumni and visitors. In order to check the authenticity of the digital diploma, it should be uploaded into the system. Then the system checks the digital signature of the file.

### **3. Drawbacks of Current Researches**

Based on what has been presented in the previous section, there are many techniques proposed for certificate verification. QR code is one of the most well-known approaches which can be used storing data for printed document authentication process. The amount of data that QR able to hold is limited and cannot include biometrics data such as the photo of the certificate holder.

Web-based authentication systems, which are connected to a database introduce high risk of database attacks to the certificate issuer. Besides, Web-based systems may affect users' privacy in addition to the cost of the network infrastructure or services providing. This type

of systems has to ensure service availability all the time, which is a big challenge for developing countries such as Libya .

Finally, most of the certificate authentication models verify the authenticity of the whole document but they do not locate tampered areas if the certificate has been tampered.

#### **4. The Proposed Model**

The proposed model consists of two processes namely: issuing and verification. The university creates and issues an electronic version of the certificate. This e-certificate is embedded with encrypted version of the university logo and the encryption key is also encrypted using the private key of the university and attached as a QR code to the e-certificate. This will insure the authenticity and the integrity of the certificate. The verification process is implemented at the certificate receiver side at which the certificate is checked and verified for authenticity purposes.

##### **4.1. Issuing Process**

e-Certificate is issued by the university in image format. It is a soft copy of paper certificate attached by barcode which contains of the encrypted key. This key is used to encrypt the university logo in order to embed it inside the image of the certificate.

The steps of preparing the e-Certificate are explained as follows:

1. Generate a soft copy of student certificate in image format.
2. Convert the image of university logo into binary image after resizing it as the certificate image size. Note that the university logo is a standard logo, because it will be used in the verification process.
3. Encrypt the binary image using 2D triangular chaotic map as described in [10].
4. The encryption key, which contains of 128 bits, is encrypted using the private key of the university.

5. A barcode of the encrypted key is generated and appended on the image produced in step 1 as required by the issuer.
6. The key used for encrypting the logo is also used to specify the pattern of embedding logo bits in one of the three color channels of each pixel in the certificate image. For example, if the key presented in hexadecimal as follows:

Key = f 8 7 f f f c b 8 6 5 2 8 b c 1

the remainder after division of each digit of the key by 3 is produced and added by one, as follows:

Embedding pattern= 1 3 2 1 1 1 1 3 3 1 3  
3 3 3 1 2

This pattern is followed to choose the channel used for embedding the logo, where 1,2 and 3 indicate red channel, green channel and blue channel, respectively. The first bit of the watermark will be concealed in the Red channel of the first pixel, while the second bit will be hidden in the Blue channel of the second pixel and etc....

7. Finally, after embedding all logo bits, the e-certificate generating process is completed and a copy of this e-certificate could be submitted to the owner.

## 4.2. Verification Process

In the verification process, the receiver of the e-certificate needs to prove that it is really originated from the issuer and to ensure that it is not tampered or modified. The issuer will make verification application available on the issuer website. This application should be installed by student or any third party. Using this application, the student or the reviewer is able to authenticate the e-certificate even if

they are offline and not connected to the university database. The verification steps are detailed as in the following:

1. The e-certificate reviewer (student or third party) will download and install the verification application from the issuer website.
2. The barcode on the e-certificate is scanned by the application to get the encrypted encryption key from it and decrypted by the public key of the university.
3. Extract the embedded binary image of the university logo from the e-certificate using the key obtained from the last step.
4. Produce binary image of university logo as in step 2 in authentication process.
5. Encrypt the binary image using the same technique in step 3 in authentication process.
6. Compare the two images produced from step 3 and step 5. if they are identical, this means that the e-certificate is authentic and not tampered. However, if they are not identical, the application could find the locations of tampering.

## **5. Experimental Results and Analysis**

In order to test the quality of the e-certificate image after embedding the logo of the university, three certificate images (C1, C2 and C3) and three transcripts (T1, T2 and T3) from three different universities are embedded with the corresponding logos (L1, L2 and L3) refer to Table.1.

**Table-1: The Test Images**

|   |   |  |
|---|---|--|
|    |    |   |
| <b>C1</b>   | <b>T1</b>   | <b>L1</b>  |
|   |   |  |
| <b>C2</b>   | <b>T2</b>   | <b>L2</b>  |
|  |  |  |
| <b>C3</b>   | <b>T3</b>   | <b>L3</b>  |

The performance of embedding the logo is evaluated in terms of embedding capacity, imperceptibility, as well as tampering detection. The peak signal-to-noise ratio (PSNR) is used to measure the visual quality of embedded images. Table.2 illustrates the results of the test images, which prove that the logo is hidden in the certificate successfully and it offers good visual quality. The visual quality of the embedded certificates is very good, where the values of the PSNR of all test images are higher 128 dB.

**Table-2: The embedding capacity (bpp) and the visual quality of the watermarked certificates**

| Image        | Logo        | PSNR       | Embedding capacity |
|--------------|-------------|------------|--------------------|
| cert1.png    | logoz.jpg   | 128.7559   | 1                  |
| Cert2.png    | logoz.jpg   | 128.748750 | 1                  |
| Scan0007.jpg | logoUTM.jpg | 128.8068   | 1                  |
| Scan0001.jpg | logoUTM.jpg | 128.7954   | 1                  |
| Scan0013.jpg | LogoUKM.png | 128.8411   | 1                  |
| Scan0005.jpg | LogoUKM.png | 129.1192   | 1                  |

Further, if the certificate is announced as not authentic, this means it is tampered with and the proposed model is able to detect the manipulated regions. To demonstrate tamper localization, we modified the watermarked certificate maliciously by replacing some certificate regions that are of educational importance. Figure 1 shows an example of detecting and localizing the tampered regions in the forged certificate.



**Figure 1: Results of verification process. (a) Original marked certificate; (b) Tampered certificate; (c) Detected tampered locations**

Moreover, the proposed model is able to provide the authenticity and integrity of e-certificates without using any network-dependent processes, which makes it an off-line and secure process that helps to reduce the risks of transmission in open environment.

## 5. Conclusion

In this paper, a new model for protecting and authenticating educational certificates is proposed. The proposed model urges educational institutions and universities to issue an electronic version of certificates and submit it to the owner. The e-certificate is generated as a copy of the paper certificate which is watermarked by the encrypted logo of the university. The encryption key is also encrypted using the private key of the university and converted to a barcode, which is attached to the e-certificate. The experimental results show that the visual quality of the generated certificate is not affected. Moreover, the viewer of the e-certificate is able to download and install the verification software from the university website. Using this software, the viewer could authenticate the source of the e-certificate and ensure its integrity. If the certificate is tampered the software can



localize the tampered areas without the need to connect to the university database and exposing users' information to the risk of disclosure.

---

## References

- [1] A. Singhal and R. Pavithr, "Degree certificate authentication using QR code and smartphone," *International Journal of Computer Applications*, vol. 120, 2015.
- [2] O. S. Sale, O. Ghazali, and Q. Al Maatouk, "Graduation certificate verification model: a preliminary study," *International Journal of Advanced Computer Science and Applications*, vol. 10, 2019.
- [3] Z. Yahya, N. S. Kamarzaman, N. Azizan, Z. Jusoh, R. Isa, M. Y. Shafazand, *et al.*, "A new academic certificate authentication using leading edge technology," in *Proceedings of the 2017 International Conference on E-commerce, E-Business and E-Government*, 2017, pp. 82-85.
- [4] R. M. Kaibiru and B. Shibwabo, "A Prototype for authentication of secondary school certificates: a case of Kenya certificate of secondary education," 2017.
- [5] H. Al-Maksousy and H. Abdulhussein, "Robust Visible Digital Stamp for Instant Documents Authentication and Verification," in *IOP Conference Series: Materials Science and Engineering*, 2020, p. 012071.
- [6] A. Husain, M. Bakhtiari, and A. Zainal, "Printed document integrity verification using barcode," *Jurnal Teknologi*, vol. 70, 2014.
- [7] V. Anitha and R. L. Velusamy, "Authentication of digital documents using secret key biometric watermarking," *International journal of communication network security*, vol. 1, 2012.
- [8] L. Chen-Wilson and D. Argles, "Towards a framework of a secure e-Qualification certificate system," in *2010 Second International Conference on Computer Modeling and Simulation*, 2010, pp. 493-500.

- [9] A. Finandhita and I. Afrianto, "Development of e-diploma system model with digital signature authentication," in *IOP Conference Series: Materials Science and Engineering*, 2018, p. 012109.
- [10] N. O. Abokhdair, A. B. A. Manaf, and M. Zamani, "Integration of chaotic map and confusion technique for color medical image encryption," in *6th International Conference on Digital Content, Multimedia Technology and its Applications*, 2010, pp. 20-23.



**Public Health and ELF Fields  
Case Study**



## **Public Health and ELF Fields Case Study**

Amer Daeri (IEEE S.M)  
Department of Computer Engineering  
University of Zawia, Zawia, Libya  
[amer.daeri@zu.edu.ly](mailto:amer.daeri@zu.edu.ly)

Ali Salah Elfalleh  
Department of Electric and Electronic Engineering  
Subratha University, Subratha, Libya  
[ali59ly@yahoo.com](mailto:ali59ly@yahoo.com)

Rajab Ibsaim  
Department of Electric and Electronic Engineering  
University of Zawia, Zawia, Libya  
[ibsaim2000@yahoo.com](mailto:ibsaim2000@yahoo.com)

### **Abstract**

As it is very well known that sources of electromagnetic fields are considered as a source of pollution. These fields as the case with any other pollutants may have some adverse effects on health, which might lead to some diseases such as cancer or childhood leukemia. These fields are classified as per the frequency range; the 50 - 60 Hz power lines are within the Extremely Low-Frequency range (>0 – 3000 Hz). The spread of power plants, switching stations, and transmission lines everywhere initiated the process of researching the possible effects that the fields associated with these electric facilities can have on human health. This work shows the field measurements results that are obtained by measuring electromagnetic fields intensity

connected to the Extremely Low-Frequency (ELF) on some chosen medium voltage lines and switching stations in various areas of Libya so to measure the Extremely Low-Frequency (ELF) to check that the measured results are compatible with the standards set by the International Commission on Non-Ionizing Radiation Protection ICNIRP. The measured values, in general, are within the limits set by the international standards.

**Keywords:** switching station – fields – health – ELF.

## **1. Introduction**

Electromagnetic fields are a factor in environmental pollution, and numerous researches have shown the impact of these fields on humans and animals on a global and regional scale. Over the past three decades, researchers have been able to get some unpleasant information about electromagnetic fields associated with power transmission lines, telecommunications equipment, radio and video broadcasting stations, among others. Research in this field is still ongoing and every time the studies come up with a proposal to reduce and take care in dealing with those fields at different frequencies and intensities. Many standards have been set by international organizations for the exposer reference limits, one of these international bodies is the Institute of Electrical and Electronic Engineers (IEEE), which published many standards for ELF fields limits [1]. Exposer to electromagnetic fields may have effects on tissues and organs of human body as well as effects associated with induced currents, electric shocks and on cardiac pacemakers plus the possible cause of cancer and child leukemia [2,3,4]. There have been many concerns among general public as well as organization regarding being close to substations or switching stations. Substations are responsible for converting from one voltage level to another and usually convert from high voltage level to consumer voltage level and



therefor they contain transformers, circuit breakers, switch gear, buses, gantries and communication equipment [5].

## **2. Related Work**

Effects of exposure to the electromagnetic fields on public and occupational health was and still is a concern for many organizations worldwide. Many researches have been conducted to assess these effects on human health. In a review [6] related to the findings of the exposure assessment studies done in Europe on the exposure of the general public to ELF fields. In this study the authors have reviewed many exposure measurements for the general public in some European countries in urban, rural, indoor and outdoor environment. This survey has indicated that the average magnetic field flux density for outdoor power lines was 0.2 micro tesla ( $\mu\text{T}$ ) and for transformer buildings and at boundary fences of substations, the maximum field flux density ranges from 20 – 80  $\mu\text{T}$ . In residential areas the major sources of magnetic field are household domestic appliances, nearby power transformers and high voltage transmission lines. The average magnetic field density was found to be 0.2  $\mu\text{T}$ . Also, the study indicated that there is a clear association between residential magnetic field intensity and the type of residence, where apartments buildings have the highest average. Regarding measurements close to transformer stations, it was found that buildings which in direct contact with transformer room have higher magnetic field intensity. The average field intensity was around 0.55  $\mu\text{T}$  for these buildings and around 0.2  $\mu\text{T}$  for buildings which are further away from transformer. The authors in [7] has simulated the effect of high voltage substation equipment on the staff at this location and they have used the Solid Works package. From their investigation, they found that in some area especially near buss bars, circuit breakers and line bays the electric field intensity was relatively high around 6 KV/m, which is still within the ICNIRP limit of 10 KV/m for

occupational exposer limit. In a study for occupational exposer in 110KV switching and transforming stations [8], the authors have made an instantaneous RMS electric and magnetic field measurements in various places within and outside these stations. The authors carried a statistical analysis for the obtained results and found out that the electric field strength did not exceed 10 KV/m in most areas except in areas near breakers and for the magnetic field most measurements were less than 500 $\mu$ T except in one place near some cables of reactor.

### 3. Measurements Method

This work is a part of a project to measure the effects of electromagnetic fields on public health due to high, medium voltage transmission lines as well as switching stations in various places in Libya. In this part measurements were made on medium voltage lines and switching stations. The measurements were made at selected distances from the center of the transmission lines. Also, these measurements were taken at different times of the day under different line load conditions, i.e. when the line is fully loaded and when it has no load. The Holaday Industries HI-3604 ELF survey meter, which has a frequency range from 30 to 2000 Hz is used for measurement in this work. The electric field measurement is done by placing the survey meter on its back on the ground, with the sensor side is underneath the electric wire of the power line so that the holding arm of the meter is in parallel with the conductors of the power line to ensure accuracy of reading and to avoid human body interference. For the magnetic field measurements, the meter is held in vertical position, so that the sensor is in perpendicular orientation with the field lines, to ensure that the maximum number of magnetic flux lines cross through the loop aperture. The human body dose not interfere with magnetic field. Measurements were only done on few selected lines due to the security problems in Libya. The ELF fields of a 30 KV transmission line with a load of 15 MW connecting the city of ALkoms and Beer-Alusta Milad an area in the east of Tripoli, which are about 100 KM

apart was measured at various distances from the center of the line and at 3, 6 10 and 15 m. Another measurement was made on a 30 KV lines loaded with 17 MW in an area in Zawia known as SaLahAldin AlQyadi at the same distances from the center of the line as for the previous line. The other measurements were made on 4 transformers, two of which are 400/220 kV plus the distribution bar and the other two are 220/30 KV at distances of 30, 60, 90 and 120 m from the transformer.

#### 4. Results

The results of the measurements made on the selected sites are shown in the following figures. Figure 1 and Figure 2 show the results obtained for the 30 KV line between Beer-Alusta Milad and Al Koms. From Figure 1 it is evident that the highest effect of the electric field was in the center of the tower, where the strength of this field was 0.318 KV / m, and from Figure 2 the magnetic field has a strength of 0.4225  $\mu$ T. The further away from the center of the tower the intensity of the two fields decreases.

As for the Salah Aldin AlQyadi 30 kV line, the measured results are shown in Figures 3 and 4. What can be seen from the measurement results for this line, that the maximum value of the electric field was 0.387 kV. In the middle of the tower, the magnetic field had the highest reading of 0.872  $\mu$ T.

From the readings obtained for the aforementioned lines, it is clear that the higher the voltage in the line, the higher the field strength. It can also be seen that the greater the distance from the center of the tower, the weaker the strength of the electric and magnetic fields. The results obtained are well below the limits set by the International Commission on Non-Ionizing Radiation Protection (ICNIRP), which are intended for the general public (5 KV/m, 160 A/m and 200 T) and for work (10 KV/m and 800 T). A/m and 1000 T).

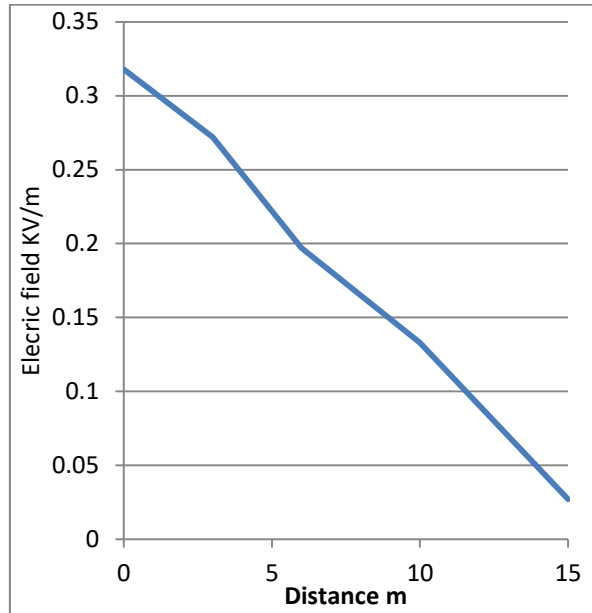


**Figure 1: Electric Field of The 30 KV Line Connecting Beer Alusta Milad and Akomes**

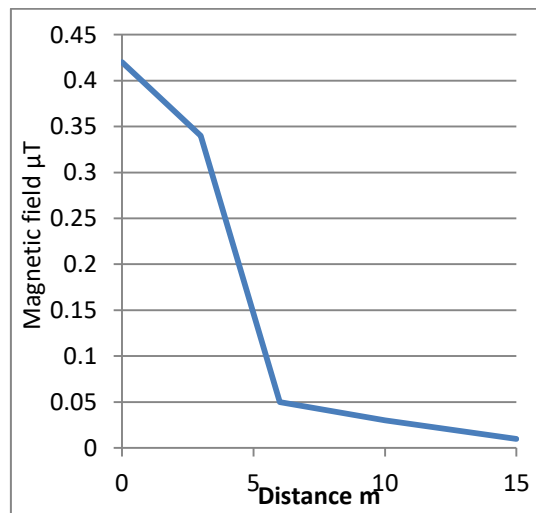


**Figure 2: Magnetic Field of The 30 KV Line Connecting Beer Alusta Milad and Akomes**

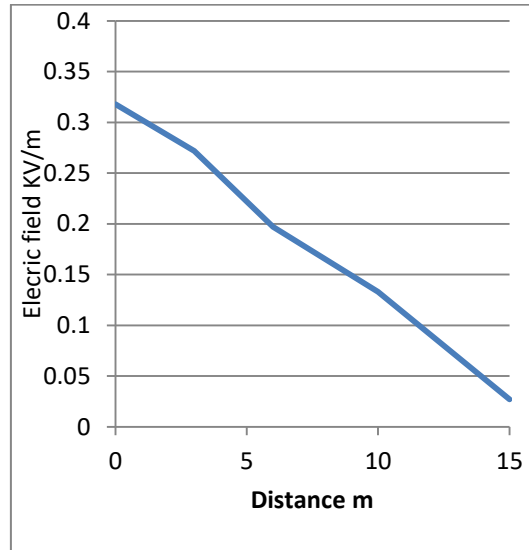


Figure 3: Electric Field for The Salah-Alden Alqiadi 30 KV Line

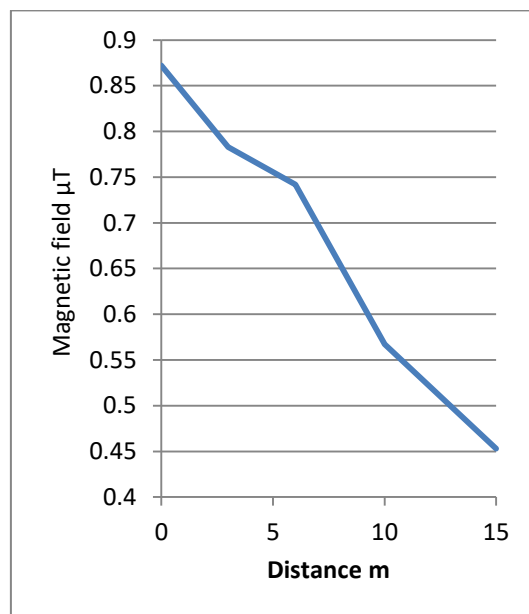
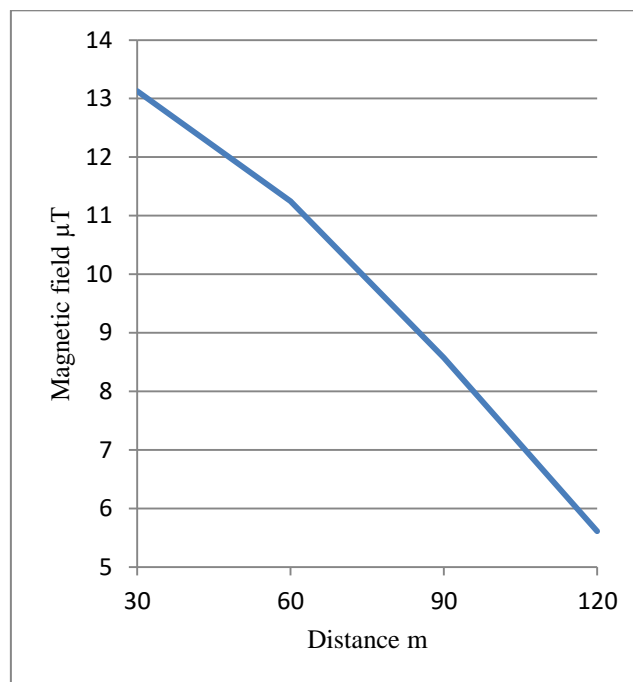
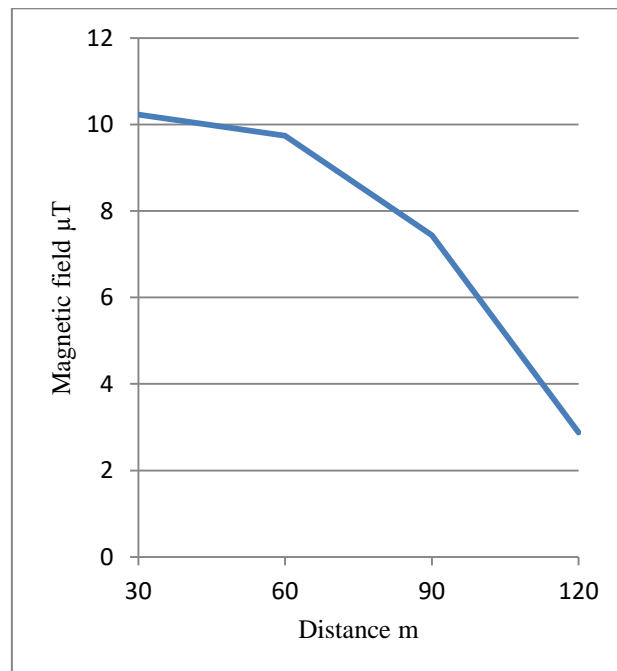


Figure 4: Electric Field for The Salah-Alden Alqiadi 30 KV Line

For the 400/220 KV transformer number 1 the greater the distance from the transformer the weaker is the field strength of the magnetic field and the highest value was 3.128  $\mu\text{T}$  at a distance of 30 cm from transformer. As for the second transformer the largest measured value was 10.225  $\mu\text{T}$  at a 30 cm distance from the transformer. Results for these two transformers can be seen in Figures 5 and 6 respectively.



**Figure 5: Magnetic Field for the 400/220 KV Transformer 1 for the Alkoms and Beer Alusta Milad Transmission Line**



**Figure 6: Magnetic Field for The 400/220 KV Transformer 2 for The Alkoms and Beer Alusta Milad Transmission Line**

The 220/30 KV transformers 1 and 2 obtained results are shown in Figures 7 and 8 respectively. From Figure 7 it is quite clear that the maximum measured value was 3.575  $\mu\text{T}$  at a distance of 30 cm from the transformer. As for the second transformer, from fig 8 it is obvious that the magnetic field has the highest measured value of 1.693  $\mu\text{T}$ .

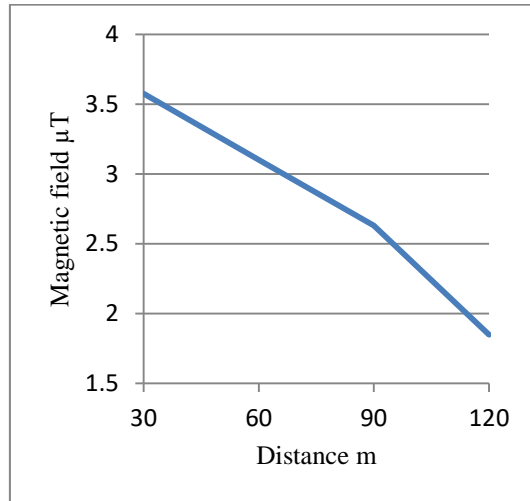


**Figure 7: Magnetic Field for The 220/30 KV Transformer 1**

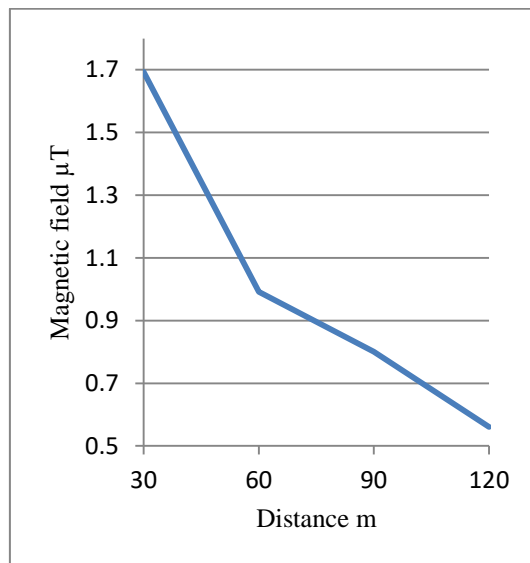


**Figure 8: Magnetic Field for The 220/30 KV Transformer 2**



## **5. Conclusion**

In this research, the results obtained through the study conducted on some medium voltage lines and transformer stations in some Libyan regions were clarified in order to determine the extent of the influence of the intensity of the electric and magnetic fields ELF resulting from these lines and the electrical transformers associated with them, and then compare these results with what it is certified by international standards. All measurements, obtained from the selected lines and switching stations, were well below the limits set by the International Commission on Non-Ionizing Radiation Protection (ICNIRP). These results indicate that there is no hazards on public health or the professionals working in the field of electricity due to exposure to these fields. Although this does not mean that caution must not be taken to be exposed to these fields for long periods since accumulation of these radiations inside the human body might lead to harmful effects and this needs further investigation.

## **ACKNOWLEDGMENT**

This work is a part of a research that was funded by Libyan Authority for Scientific Research and Technology Sciences, Tripoli, Libya grant agreement no. 282891.

## References

- [1] IEEE International Committee on Electromagnetic Safety (SCC39) "IEEE Standard for Military Workplaces—Force Health Protection Regarding Personnel Exposure to Electric, Magnetic, and Electromagnetic Fields, 0 Hz to 300 GHz PG&E's Lakeville-Sonoma 115 kV Transmission Line Project B-8, ESA / 204202, (A.04-11-011) Final Mitigated Negative Declaration", IEEE Std C95.1-2345™-2014
- [2] Asher R. Sheppard, "Health Issues Related to the Static and Power-Frequency Electric and Magnetic Fields (EMFs) of the Soitec Solar Energy Farms", Asher Sheppard Consulting Santa Rosa, California, April 30, 2014
- [3] Einat Kapri-Pardesa Tamar Hanocha Galia Maik-Rachlinea Manuel Murbach Patricia L. Bounds Niels Kuster Ronny Seger, "Activation of Signaling Cascades by Weak Extremely Low Frequency Electromagnetic Fields", Published by S. Karger AG, Basel, 2017.
- [4] Madar Talibov et. al., "Parental occupational exposure to low-frequency magnetic fields and risk of leukaemia in the offspring: findings from the childhood Leukaemia International Consortium (CLIC)", *Occup Environ Med* 2019;76:746-753.
- [5] David Black, "Health Effects Assessment", Genesis Energy Ltd, June 2011.
- [6] Peter Gajšek, Paolo Ravazzani, James Grellier, Theodoros Samaras, József Bakos and György Thuróczy "Review of Studies Concerning Electromagnetic Field (EMF) Exposure Assessment in Europe: Low Frequency Fields (50 Hz–100 kHz)", *International Journal of Environmental Research Public Health* 2016, 13, 875.
- [7] Calin Munteanu, Marius Purcar, Dan Bursasiu, Emil Merdan, Vasile Farcas, "CAD/CAE Modeling of the Human Exposure

to Electric Field Inside a High Voltage Substation", International Conference and Exposition on Electrical and Power Engineering (EPE 2014), 16-18 October, 2014, Iasi, Romania.

- [8] LEENA KORPINEN<sup>1\*</sup>, HARRI KUISTI<sup>2</sup>, AUNO PA<sup>^</sup>A<sup>^</sup>KKO<sup>^</sup> NEN<sup>3</sup>, PAULI VANHALA<sup>4</sup> and JARMO ELOVAARA<sup>2</sup>, " Occupational Exposure to Electric and Magnetic Fields While Working at Switching and Transforming Stations of 110 kV", Ann. Occup. Hyg., Vol. 55, No. 5, pp. 526–536, 2011.





**Effect of Dust Storm on WiMAX System  
in Libyan Desert Environment**

**4**



## Effect of Dust Storm on WiMAX System in Libyan Desert Environment

Nadia Aboalgasm

College of Technology Engineering Janzour, Libya

[nadia\\_mo2003@yahoo.com](mailto:nadia_mo2003@yahoo.com)

Ftah Nuri

Libyan Academy, Tripoli

[raingiki@gmail.com](mailto:raingiki@gmail.com)

Ahmed M Belghasem

College of Renewable Energy Tajoura-libya

[belghasemahmed@gmail.com](mailto:belghasemahmed@gmail.com)

### **Abstract**

Signal attenuation is an important parameter in telecommunications applications because of its importance in determining signal strength as a function of distance. A major cause of this phenomenon is atmospheric particles which can seriously limit the performance of telecommunication system especially at microwave level.

Dust storms occur in many parts of the world, especially in the African Sahara, Middle East. During the storm, dust particles raise high enough above the earth's surface to lie within the path of microwave radio links causing a Loss of Signal Energy and Resulting in Service degradation. In this paper the effect of the dust storms on the World interoperability for Microwave access(WiMAX) systems in southern region of Libya is studied by adopting a dust storm simulation model which depends on many variables such as frequency, visibility, particles-size and complex permittivity specified for the Libyan desert, using this model can simulate various dust storm severities in terms of the visibility, by adding a communication

block to be used as a channel effect (noise injection) within Additive White Gaussian Noise (AWGN) channel in complete WiMAX communication system that deploys several digital modulation schemes. The obtained results show that the effect of dust storm on the WiMAX system is very severe and this effect increases as frequency increases.

**Keywords:** Dust - Storm - AWGN - Frequency – Visibility – Particle Size – Attenuation - WiMAX.

## **1. Introduction**

Wireless broadband is a technology which has the capability to provide instantaneous bandwidth and high data rates over a wide coverage area. The technology operates in line-of-sight (LOS) configurations, where the Base Station (BS) and subscriber station (SS) have a clear view of each other and non-line-of-sight (NLOS) configurations, where the radio transmission path is partially obscured. LOS configurations are estimated to have a range of up to 50km and achieve download speeds of over 100 Mbit/s. NLOS configurations, on the other hand, communicate in a much smaller range and are able to achieve lower data rates, depending on the level of obscuration [1].

WiMAX networks are widely used in many locations in Libya, whether in the big cities or in the scattered desert sites, especially oil field's locations.

Environment has a great effect on the WiMAX network performance, one of the environmental parameters that have an effect and not being paid more attention is the sand storms. Sand storms affect the performance of the wireless communication due to the amount of dust in general, which in turn magnifies the fading effect and since Libya is considered as desertification country. In the last few years many problems in wireless communication networks have been recorded in windy and sandy days in the southern part of Libya; No scientific



reason has been given for these problems. Wind storms may last for days, reducing visibility to just tens of meters or as little as few meters [1].

The effect of dust particles on signal attenuation received considerable attention especially at high frequencies [2].

As most of the work done in this area was carried out in Europe and USA, a significant amount of research has been done in developing models to quantify the impact of rain and snow attenuation on communications systems operating in the microwave region [3]. In contrast of that, little work has been done to investigate the impact of dust storm on the same propagation paths [3]. Rapid development in telecommunication technology and increasing competition in the sector has extended service to new locations and environments especially in Africa and Asia.

## **2. Related Work**

Many studies have been conducted regarding the dust storms effect on the communication systems. In [1] the effect of sand and dust storms on wireless communication in the southern region of Libya (Sebha, shati, Obari, Morzok, Ghat) evaluated. These places were chosen for collecting the sand and dust in order to be analyzed and compared with the climate conditions to estimate the factors which are needed for calculating the effect of dust storms on GSM networks and microwave links. The results of this study showed that the GSM Signal coverage attenuation, due to dust storms with low visibility and with low humidity < 60% is negligible at any height for cells, while the attenuation at humidity (H) =100% is serious at any height. For the microwave signal attenuation due to dust storms with low visibility and low or high humidity are serious at any height.

Similarly, in study [3] presented a mathematical model developed to predict the microwave signal attenuation due to dust storm. The proposed model enables the convenient calculation of the microwave signal path attenuation which relates visibility, frequency, particle size

and complex permittivity of dust storm then the predicted values from the mathematical model are compared with the measured values observed in Sudan and Saudi Arabia which showed a relatively close agreement. The results show that the attenuation is varying from 13 to 0.2 dB/km at 40 GHz for dust particle radius equal to 50 $\mu$ m as the visibility varies between 10 to 500m. While at higher frequency of the band (100 GHz) the attenuation is varying from 47 to 2 dB/km for dust particle radius equal to 50 $\mu$ m as the visibility varies between 10 to 500m.

Another research proposes an empirical model to predict the attenuation due to dust storms based on a one-year measurement of visibility, humidity and their effects on microwave links in Sudan. Signal strength variations on two operational microwave links at 14 GHz and 22 GHz as well as visibility were monitored simultaneously. The model is developed empirically using measured attenuation and measured storm characteristics (e.g., visibility, dielectric constant, frequency and moisture content). The predicted attenuation from the proposed empirical model was compared with the attenuation at frequencies ranging from 7.5 GHz to 40 GHz measured at different locations, and good agreement was found [4].

In reference [5] a dust storm is modeled as circularly symmetric having a visibility with a minimum at its center (e.g., maximum mass loading) and which exponentially increases radially to a fixed maximum visibility threshold level (minimum mass loading). This model enables the convenient calculation of the two-dimensional (2-D) structure of radar backscatter and path attenuation. As an example, the parameters of the exponential function describing the visibility distribution for a particular dust storm was derived using measurements made in the Sudan by other investigators operating a 10.5 GHz, 25 km link. A comparison of the calculated and measured attenuation time-series showed relatively close agreement.

Most of the mentioned studies were concerned with modeling of a dust storm model and its effect on the wireless communication in

general or just studying the model itself on different frequency bands or different regions with different moisture content and humidity levels but no application for this model on a certain telecom system was detected.

In this paper a dust storm model is used and applied in WiMAX system taking into account Libyan desert conditions as per [1] and studied its performance and behavior under a specific dust storm with multiple modulation types channel bandwidth's, Cyclic Prefix (CP's) and tower heights.

### 3. Simulation and Results

Table 1 summaries the used dust conditions in the south of Libya which were used to evaluate the attenuation effect on WiMAX system.

**Table-1: Dust Model Parameters**

| Parameter              | Value                    |
|------------------------|--------------------------|
| maximum temperature    | 45 c <sup>o</sup>        |
| Wind speed             | 10 - 22km/h              |
| Proportion of rainfall | 0-3.4mm                  |
| Average density        | 2.5764 g/cm <sup>3</sup> |

The complex permittivity is calculated from equation 1.

$$\varepsilon' = 6.3485 + 0.04H - 7.78 \times 10^{-4}H^2 + 5.56 \times 10^{-6}H^3 \quad (1)$$

$$\varepsilon'' = 0.0929 + 0.02H - 3.71 \times 10^{-4}H^2 + 2.76 \times 10^{-6}H^3$$

Where:

$\varepsilon'$ : Real part of complex permittivity

$\varepsilon''$ : Imaginary part of complex permittivity

$H$ : humidity, it assumed to be 0% as it is desert area.

The mathematical dust model obtained by Samir I.Ghobrial [6] using an analysis based on the work of Maxwell Garnett used is shown in equation 2.

$$\alpha = \frac{2.46 \cdot 10^{-5} \cdot v}{\lambda} * \frac{\epsilon''}{[(\epsilon' + 2)^2 + (\epsilon''^2)]} \quad (2)$$

Where:

$\alpha$ : attenuation per km.

$\lambda$ : Frequency.

$v$ : Relative volume occupied by particles.

The relative volume occupied by particles was calculated using equation 3

$$v = \frac{c}{\rho * V\gamma} \quad (3)$$

Where:

$\rho$ : Density of dust.

$\gamma, c$ : Constants depend on distance from the point of origin of dust storm with the values  $2.3 \times 10^{-5}$ . And 1.07 respectively.

$V$ : visibility.

The visibility during dust and/or sand storms was calculated using equation 4:

$$V\gamma = \frac{c * h^b}{a} \quad (4)$$

Where:

$a$ ,  $b$  constants depend on dust particles size distribution, geographical and climatic conditions.

$h$ : height of tower.

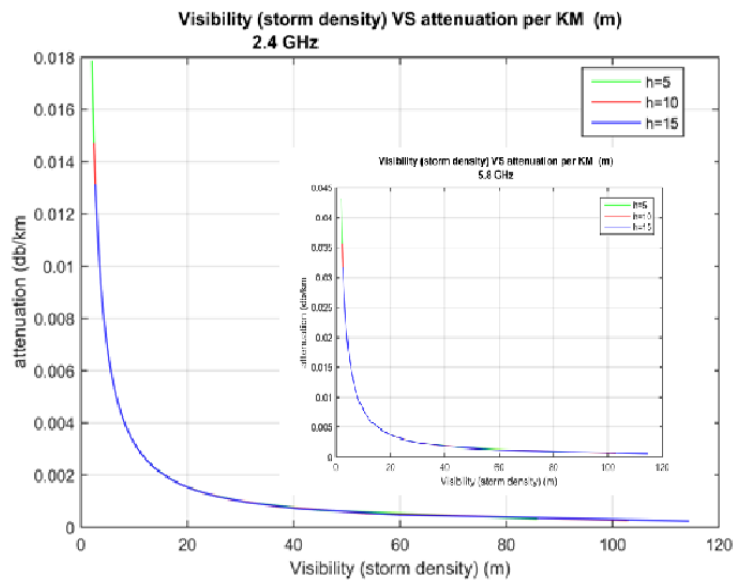
The model output is the amount of attenuation introduced by dust storm which will be added to the channel parameters in the WiMAX system block as a noise to be able to study the effect of the storm on the Bit Error Rate (BER).

Table 2 details the different parameters that were used to carry out the simulation.

**Table 2: Simulation Parameters**

| Parameter         | Value                             |
|-------------------|-----------------------------------|
| Frequency         | 2.4 and 5.8 GHz                   |
| Channel           | AWGN                              |
| Modulation        | QPSK, BPSKM, 4QAM and 16QAM       |
| Bandwidth         | 1.25, 2.5, 5, 10,15,20 and 28 MHz |
| Cyclic prefix     | 1/4, 1/8, 1/16, 1/32              |
| Tower height      | 5, 10, 15 meters                  |
| Coverage distance | 5 km                              |
| Symbol rate       | 10                                |

The first test for testing the visibility on the attenuation for 2.4 and 5.8GHz with three tower height as shown in Figure 1.



**Figure 1: Effect of visibility on the attenuation at different heights**

The results showed that the 5.8GHz is more affected by dust storm model compared with 2.4GHz, whereas the storm severity remains fixed (visibility is fixed) it was noticed that the attenuation per KM is much higher, for example, for the 5 meter height with visibility of 85.7 meters the attenuation was 0.00032 db\km for the 2.4GHz but for the 5.8 GHz at the same visibility (85.7 meters), the attenuation was 0.00078 db\km which means around 143% increase in the attenuation per km for the selected storm (85.7 meters) if operating frequency is 5.8GHz instead of 2.4GHz.(In other words. The attenuation increases by frequency increase).

The second test for testing the tower height effect on the attenuation with assumed a fixed dust storm intensity factor  $a=0.007$  and an operating frequency as shown in Figure 2.

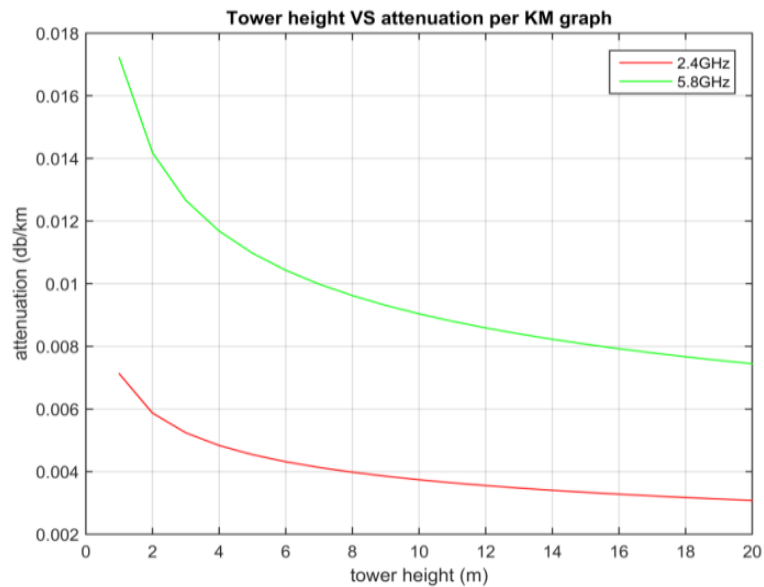


**Figure 2: Effect tower height on the attenuation**

It can be noticed that as the height increases the attenuation decreases due to the distance increase from the earth surface as the dust particles originating there when a storm is happening.

Also the frequency effect observation still applies as the 5.8GHz is more affected by the storms, for example, at height 10 meter, it is clear from obtained results that the visibility is the same (8.725202403 meter) as it is a function of the storm severity factor ( $a$ ) and not the frequency, so we get 0.003739856 db/km for the 2.4GHz and 0.009037985 db/km for the 5.8GHz.

The third test for testing Effect of dust storms on the WiMAX 802.16 performance with different modulation schemes.

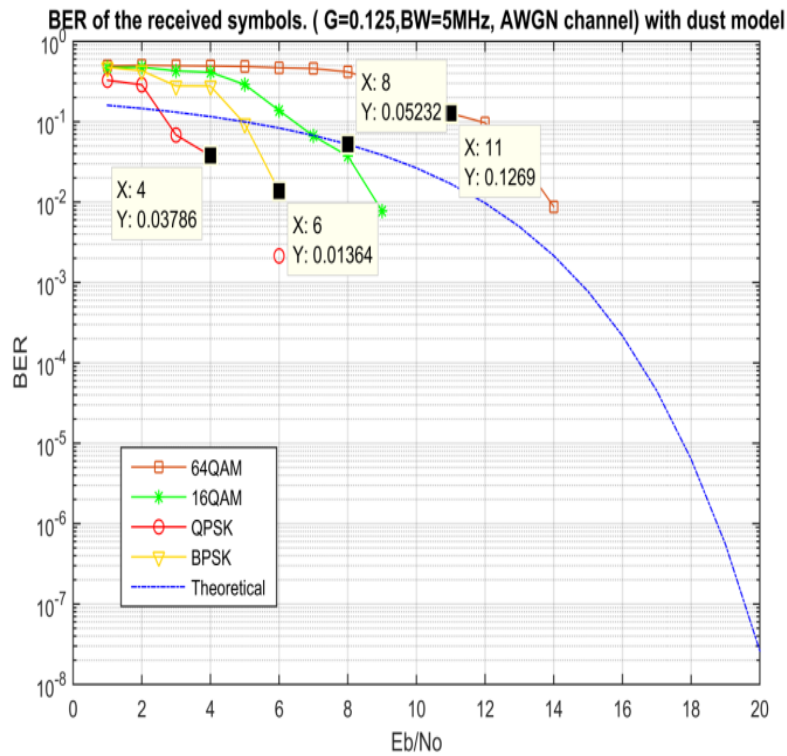


**Figure 3: BER vs SNR graph for different modulation**

From the obtained results indicated in figures (3) it is clear that when working at dusty environments, with the system specification mentioned, it is better to work with the QPSK schemes.

The fourth test for testing Effect of dust storms on the WiMAX 802.16 performance with different cyclic prefix size.



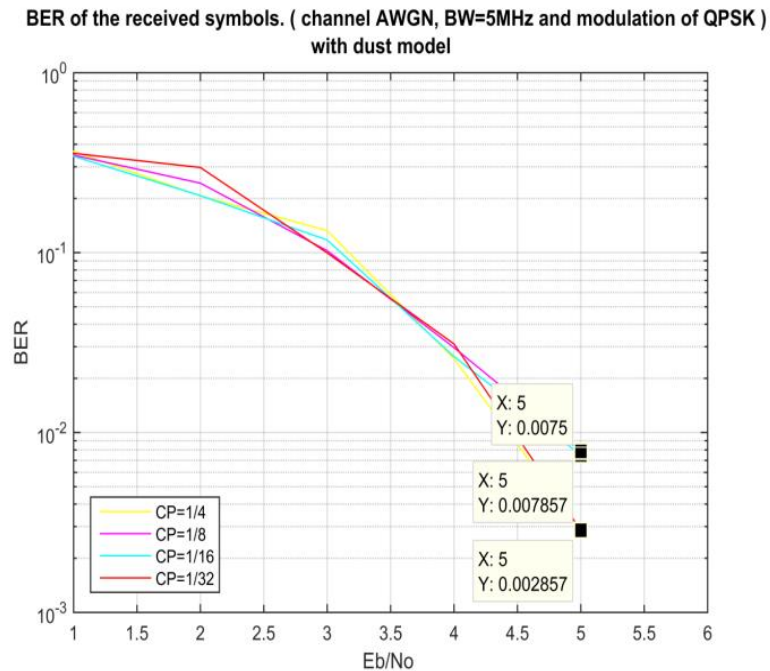


**Figure 4: BER vs SNR graph for cyclic prefix**

It is well noticed from figures (4) that the dust storms can also affect the system regardless of the CP size, just the difference is the magnitude of this effect on the different CP sizes, for example it can be noticed that for the CP sizes (1/32 and 1/8) the biggest increase of the BER when the dust storm striking around 170% and 700% respectively but for the 1/16 and 1/4 the biggest increase is by 1900% and 2000% respectively. So, can be said that (1/8 and 1/32) are better than the other two.

Finally testing effect of dust storms on the WiMAX 802.16 performance with different channel bandwidths (BW) with appropriate parameters based on previous results.

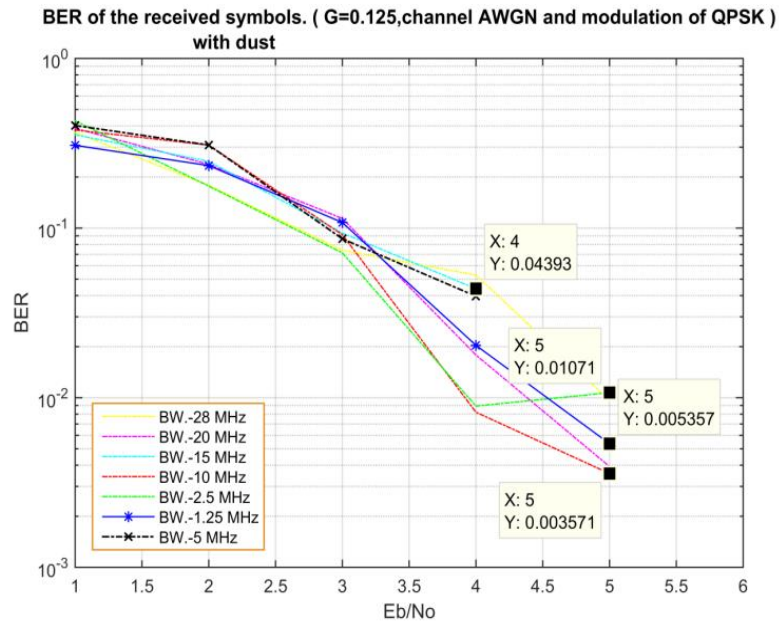


**Figure 5: BER vs SNR graph for different channel bandwidths**

It can be noticed from the obtained results Figure 5 that each BW has different behavior and no particular pattern had been spotted but in general it can be said that it is not necessary to the system to be more affected with storms just because it has a higher channel BW but it is a factor.

The used 5MHz channel in this study showed a good result an acceptable BER will require  $E_b/N_0 = 4.5$  db or higher along with the 15MHz channel, the other channel BEs will need more than the 5db to achieve an acceptable BER.

#### 4. Conclusion

This paper presented an effect of the dust storms on the simulated WiMAX systems in southern region of Libya by proposing a dust storm simulated model which depends on many variables such as frequency, visibility, particles-size and complex permittivity specified for the Libyan Desert.

Many tests were setup using Matlab software in order to evaluate the effect of dust storm on the WiMAX performance in term of BER. The BER performance was measured against SNR considering modulation schemes, tower heights, Cyclic prefix values and bandwidth. The results show that as the storm severity increases the attenuation increases. This increase varies based on the involved system parameters such as modulation type, CP value and tower height although from the results bandwidth variation doesn't have a major effect but it is a factor to be considered.

The final conclusion is that sand storms have some effect on WiMAX system performance but this effect can be partially mitigated by careful choice of system components and parameters such as frequency, tower height and modulation scheme.

The results show that most suitable modulation scheme is QPSK from BER point of view as it has the lowest BER with lowest SNR with acceptable data rate.

The lower frequency the better the BER. The effect of CP and BW wasn't significant and hence they don't have a major effect.

## **References**

- [1] EM. Abuhdima, IM. Saleh, “Effect of sand and dust storm on Microwave propagation signals in southern Libya” ; Melecon 2010-2010 15thIEEE Mediterranean Electrotechnical Conference; 2010 ; pp.695-698.
- [2] Z. Alabdin, Md. Rafiqul Islam, O Othman. Khalifa, Hany Essm A Raouf, Momoh Jimoh E Salami,”Development of Nathematical Model for the prediction of Microwave Signal Attenuation due Dust storm”, Proceeding of the International Conference on Computer and Communication Engineering 2008, May 13-15, 2008 Kuala Lumpur, Malaysia.
- [3] “IEEE Standard for Local and metropolitan area network Part 16: Air Interface for Broadband Wireless Access System Amendment 1: Multiple Relay Specification”, IEEE Std802.16j-2009(Amendment to IEEE Std 802.16-2009), pp.c1-290, June 12, 2009.
- [4] P. Iyer, Nat. Natarajan, M. Vencatachalam, A. Bedekar, E. Gonen, K. Etemad, P. Taaghoh; “All-IP network architecture for mobile WiMax”; 2007 IEEE Mobile WiMax Symposium; pp.54-59, March 25-29-2007.
- [5] Ifat Rashid, “Performance comparison of Rayleigh and Rician fading Channel Models: A Review”, International Journal of Advance Engineering and Research Development, volume 5, Issue 02, February-2018.
- [6] S.I Ghobrial and S.M Shrief; "Microwave Attenuation and Cross-Polarization in Dust Storms", IEEE Trans on Ant. And prog. ,vol.AP-35,No.4, 1987, pp 418-425.



**Optimizing Submerged ARC Welding  
Process Variables Using Taguchi Method**

**5**



## Optimizing Submerged ARC Welding Process Variables Using Taguchi Method

Abdulbaset A. Frefer

Mechanical and Industrial Engineering Department

University of Tripoli, Tripoli, Libya

[a.frefer@uot.edu.ly](mailto:a.frefer@uot.edu.ly)

Al-Sonosi. M. Abohusina

Department. of Mechanical Engineering and Energies

Libyan Academy for Postgraduate Studies, Janzur, Libya

[amabo1961@yahoo.com](mailto:amabo1961@yahoo.com)

### Abstract

This paper investigates submerged arc welding (SAW) process variables on the quality of the weld bead geometry parameters and identifying the optimum process variables (current (I), voltage (V), and speed (S)). The experimentation is conducted for (Fe-0.137C-0.483Mn-0.356Si) in wt.% steel using bead-on-plate (BOP) technique. To determine the significant effect of these variables on achieving the desired weld bead quality (W, R, P), the researchers employed the orthogonal array for Taguchi L9 to reduce the number of the necessary experimental results for signal-to-noise ratio (S/N) calculations. The signal-to-noise ratios and the mean of the (S/N) ratios of the output responses are calculated to determine the optimum process variables. Analysis of Variance (ANOVA) is used to assess the impact of welding process variables on the characteristics of the weld bead parameters and the percentage contribution (PeC) of each variable. Experimental results revealed that the optimum levels for each of the response parameters in this study are (I1V1S3) for bead width (W), (I3V3S3) for bead reinforcement (R), and (I3V2S3) for bead penetration (P). The ANOVA analysis results indicated that the

welding current contributed significantly out of the three process variables used, especially with regard to width and penetration, followed by the welding speed. However, for the reinforcement, the PeC of the arc voltage is the highest, followed by the welding current and welding speed.

**Keywords:** SAW - Taguchi L9 orthogonal array design - S/N ratio - ANOVA and F-Test.

## **1. Introduction**

Submerged arc welding is preferred over other welding processes because it provides many advantages. Some of these advantages are deeper penetration, higher deposition rate, excellent surface appearance, high melting efficiency, availability in automatic or semi-automatic mode, improved safety, lower welder skill requirement, and high-quality welds. Due to these advantages, this process has found many applications, both for relatively thin sheets and thick plates, include the fabrication of pressure and marine vessels, tanks, bridges, shipbuilding, oil/gas pipelines, and surfacing. This welding process can weld ferrous and nonferrous metals and alloys such as low carbon, low alloy steels, stainless steels, Ni, and Ti [1-4].

Generally, the submerged arc welding process obtains a welded joint with the desired weld bead parameters and excellent mechanical properties with minimum distortion. Welding variables have a significant influence in determining the quality of a weld joint; therefore, it is essential to study the stability of these variables to achieve high-quality weld characteristics with optimum mechanical properties [5]. These variables include current, voltage, speed, nozzle-to-plate distance, wire feed rate, flux type, and plate thickness [6-9].



Many studies have investigated the selection of welding process variables and the determination of their optimum effects on weld bead characteristics (bead width, bead reinforcement, bead penetration) and mechanical properties, such as (hardness, UTS, impact, yield strength, bending, toughness) by methods such as Taguchi [10-14], Taguchi coupled with grey relational analysis [15], Taguchi coupled with utility theory [16], regression analysis [17], Taguchi and regression analysis [3][9][18], response surface methodology [6], regression and sensitivity analysis [5], regression analysis, response surface methodology and genetic algorithm [8], regression analysis, desirability approach, genetic and jay algorithms [7]. The reported results of these studies are different from each other, and this is due to the various tested material and welding variables selected. Since welding variables greatly influence the quality of a weld joint, even small changes in these variables may cause unexpected output results and welding performance [5].

The main objectives of this study are to determine the impact of submerged arc welding process variables; current (I), voltage (V), and speed (S) on the weld bead geometry bead penetration (P), bead reinforcement (R), and bead width (W) using bead-on-plate (BOP) technique of (Fe-0.137C-0.483Mn-0.356Si) in wt.% steel and to determine the optimal welding variables to yield the desired weld bead quality.

The orthogonal array (OR) for Taguchi L9 design of experiments (DOE) is employed to reduce the number of the necessary experimental runs with results comparable to a full factorial experiment [19]. Signal to noise (S/N) ratios and mean (S/N) ratios analyses are used to find the significant effects of the selected variables used on the output parameters (responses) and improving the SAW process performance within the experimental field. ANOVA is applied to estimate the most significant process variables contributing to optimum bead qualities [9].

## 2. Experimental Work

### 2.1 Equipment and Material

In this study, a semi-automatic submerged arc welding machine is made by Sweden ESAB (Elektriska Svetsnings-Aktiebolaget), the English translation is (Electric Welding Limited) company. A constant-voltage and direct-current power source are employed with a 3.2mm diameter copper-coated wire electrode in a coil form equivalent to (DIN 8557-S1) specification produced by ESAB company. The chemical composition of this electrode is shown in Table 1. The overhanging length of the electrode beyond the nozzle is 25mm. The distance between the electrode tip and the workpiece is 3mm, submerged under a layer of basic fluoride type granular flux equivalent to N.F. (A81-319) FP/B 34/23 ARI specification keeping the electrode positive polarity.

The as-received material used in this study is a steel plate with a thickness of 10mm. It has a chemical composition, as shown in Table 2. The bead-on-plate technique is used. Welds are deposited on samples in a rectangular shape with dimensions of 500×100×10mm.

**Table 1. Composition of the wire electrode**

| Element wt. %  | C    | Mn  | Si   | S    | P    | Cu   |
|----------------|------|-----|------|------|------|------|
| Wire Electrode | 0.09 | 0.5 | 0.01 | 0.05 | 0.03 | 0.20 |

**Table 2. Composition of the as-received material**

| Element | C     | Mn    | Si    | P     | S     | Ni    | Cr    | Mo    | Cu    | Fe     |
|---------|-------|-------|-------|-------|-------|-------|-------|-------|-------|--------|
| Wt.%    | 0.137 | 0.483 | 0.356 | 0.024 | 0.038 | 0.088 | 0.119 | 0.008 | 0.097 | 98.650 |

### Selection of Process Variables and Design of OA for Taguchi DOE

Table 3 presents the values of the selected welding process variables and their different levels, while Figure 1 shows weld bead geometry characteristics.

**Table 3. Welding process variables and their levels**

| Welding process variable | Unit    | Levels of the variable |     |     |
|--------------------------|---------|------------------------|-----|-----|
|                          |         | 1                      | 2   | 3   |
| Welding current (I)      | Ampere  | 350                    | 450 | 550 |
| Arc voltage (V)          | Voltage | 26                     | 27  | 28  |
| Welding speed (S)        | mm/min  | 400                    | 500 | 600 |

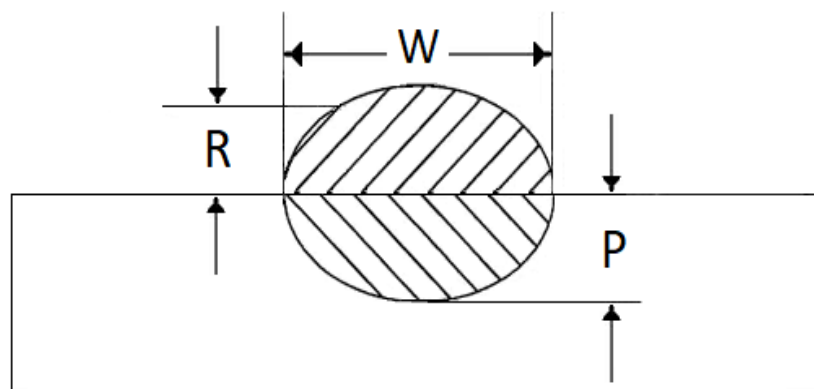


**Figure 1: Weld bead geometry characteristics**

After the performance of the welding process, cross-sections of the welds were cut, and samples were prepared using the standard method; then, the weld bead geometry characteristics are measured by the micro-dimensions up to micrometer of type Nikon V12 microscope. Welding conditions according to Taguchi design are presented in Table 4.

**Table 4. OA L9 (3<sup>3</sup>) for Taguchi DOE and welding conditions**

| Exp. No. | L9 ( 3 <sup>3</sup> ) |   |   | Welding conditions |    |     |
|----------|-----------------------|---|---|--------------------|----|-----|
|          |                       |   |   | I                  | V  | S   |
| 1        | 1                     | 1 | 1 | 350                | 26 | 400 |
| 2        | 1                     | 2 | 2 | 350                | 27 | 500 |
| 3        | 1                     | 3 | 3 | 350                | 28 | 600 |
| 4        | 2                     | 1 | 2 | 450                | 26 | 500 |
| 5        | 2                     | 2 | 3 | 450                | 27 | 600 |
| 6        | 2                     | 3 | 1 | 450                | 28 | 400 |
| 7        | 3                     | 1 | 3 | 550                | 26 | 600 |
| 8        | 3                     | 2 | 1 | 550                | 27 | 400 |
| 9        | 3                     | 3 | 2 | 550                | 28 | 500 |

## 2.2 Analysis of (S/N) Ratios:

In the Taguchi method, (S/N) ratios determine the number of performance variations from the desired values (Ross 1988). The control variables that may contribute to improved quality can be quickly identified by the number of variations present as a response.

In this study, the analysis of the (S/N) ratios are applied for only nine experiments according to Taguchi L9 (3<sup>3</sup>) DOE. All the interactions between the welding variables are neglected.

There are three categories of performance in the analysis of the (S/N) ratios: (a) lower-is-better (LB), (b) higher-is-better (HB), and nominal-is-best (NB). In this study, the output parameters (responses), namely, bead width (W) and bead reinforcement (R), belong to the quality characteristic of the lower-is-better type and bead penetration (P) belongs to the quality characteristic of the higher-is-better type. Equations 1 and 2 are used to compute the values of (LB) and (HB), respectively [19-20] [9].

For lower-the-better (LB) type, the following equation is used:

$$\text{signal-to-noise ratio (LB)} = -10 \log \left[ \frac{1}{n} \sum_{i=1}^n Y_i^2 \right] \quad (1)$$

For higher-the-better (HB) type, the following equation is used:

$$\text{signal-to-noise ratio (HB)} = -10 \log \left[ \frac{1}{n} \sum_{i=1}^n 1 / Y_i^2 \right] \quad (2)$$

Where n is the number of experiments and  $Y_i$  is the  $i^{\text{th}}$  experimental value for the performance characteristic. In this study,  $Y_i$  represents the bead geometry characteristics (W, R, P).

### 2.3 Mean of the Signal-to-Noise (S/N) Ratio:

After finding the values of the (S/N) ratios, the mean S/N ratios at each level for various variables are calculated, and graphs are drawn. The optimal levels are determined from the highest values of the mean S/N ratios among levels of the variables [9].

### 2.4 Analysis of Variance (ANOVA) According to Orthogonal Array L9(3<sup>3</sup>):

For analyzing the significant effect of the welding process variables on the response of the output bead parameters, ANOVA is used to investigate which process variables significantly affect the performance characteristic (bead geometry). This analysis is carried out for a level of significance of 0.05 for a level of confidence of 95%.

The analysis of variance can be accomplished based on the total sum of squares (SS)<sub>T</sub> from the total mean of the (S/N) ratio according to equation (3):

$$(\text{SS})_T = \sum_{i=1}^n (S/N)_i^2 - \frac{1}{n} \left[ \sum_{i=1}^n (S/N)_i \right]^2 \quad (3)$$

Where n represents all the experiment runs and (S/N)<sub>i</sub> is the calculated signal-to-noise ratio value of the  $i^{\text{th}}$  quality characteristic.

(SS)<sub>T</sub> decomposed into the sum of squares due to each tested variable (SS)<sub>f</sub> and the sum of squares due to the error (SS)<sub>e</sub>, which can be expressed by equations (4) and (5):

$$(SS)_f = \sum_{j=1}^h \frac{((S/N)_j)^2}{h} - \frac{1}{n} [\sum_{i=1}^n (S/N)_i]^2 \quad (4)$$

$$(SS)_e = (SS)_T - \sum (SS)_f \quad (5)$$

Where j is the level number of the specific variable and h is the repetition of each variable's levels. The degree of freedom (DF) due to error is calculated by using equation (6):

$$(DF)_e = (DF)_T - \sum (DF)_f \quad (6)$$

The variance for each factor is calculated by using equation (7):

$$(V)_f = (SS)_f / (DF)_f \quad (7)$$

The variance due to error is calculated using equation (8):

$$(V)_e = (SS)_e / (DF)_e \quad (8)$$

The expected sum of the squares for each variable  $(\widetilde{SS})_f$  is given by equation (9):

$$(\widetilde{SS})_f = (SS)_f - ((DF)_f \cdot (V)_e) \quad (9)$$

The Fisher test (F) determines which process variables statistically significantly affect the performance characteristic. The large value of the F-test means that the effect is great on the performance characteristic due to the change of the process variables. The F-test can be expressed by equation (10):

$$\mathbf{F\text{-value}} = (\mathbf{V})_f / (\mathbf{V})_e \quad (10)$$

The percentage contribution (PeC) for each variable can be used to evaluate the importance of each variable on the performance characteristic and can be expressed by equation (11):

$$\mathbf{PeC} = \frac{(\mathbf{SS})_f}{(\mathbf{SS})_T} \times \mathbf{100} \quad (11)$$

Equations (1 to 11) used to calculate the S/N ratios and ANOVA analysis can be found in many reported literature references such as [19-20][9]. In this study, the experimental design and the calculations are conducted with EXCEL and SPSS software applications.

### 3. Results and Discussion

#### 3.1 Results

##### Analysis of the Signal-to-Noise (S/N) Ratio:

The measured bead characteristics and the signal-to-noise (S/N) ratio values according to the loss function for the three bead characteristics are shown in Table 5.

**Table 5: Bead (P, R, W) and S/N ratios according to OA L9 (3<sup>3</sup>)**

| Exp No. | I   | V  | S   | W (mm) | (S/N) ratio | R (mm) | (S/N) ratio | P (mm) | (S/N) ratio |
|---------|-----|----|-----|--------|-------------|--------|-------------|--------|-------------|
| 1       | 350 | 26 | 400 | 15.500 | 23.806-     | 3.800  | 11.596-     | 4.840  | 13.697      |
| 2       | 350 | 27 | 500 | 15.310 | 0023.7-     | 3.250  | 10.223-     | 5.150  | 14.236      |
| 3       | 350 | 28 | 600 | 13.215 | 22.421-     | 2.160  | 6.679-      | 5.015  | 14.005      |
| 4       | 450 | 26 | 500 | 18.955 | 25.555-     | 3.275  | 10.304-     | 5.215  | 14.345      |
| 5       | 450 | 27 | 600 | 15.600 | 23.863-     | 2.315  | 7.288-      | 5.650  | 15.041      |
| 6       | 450 | 28 | 400 | 22.890 | 27.193-     | 2.590  | 8.264-      | 5.000  | 13.978      |
| 7       | 550 | 26 | 600 | 18.060 | 25.134-     | 2.480  | 7.876-      | 6.180  | 15.820      |
| 8       | 550 | 27 | 400 | 25.000 | 27.959-     | 2.740  | 8.752-      | 5.860  | 15.357      |
| 9       | 550 | 28 | 500 | 23.720 | 27.502-     | 1.800  | 5.097-      | 5.720  | 15.145      |

**Mean (S/N) Ratios:**

The most significant value of the mean (S/N) ratios for the three levels for each of the process variables is the optimum because a high value of signal-to-noise ratio indicates that the signal is much higher than the random effects of the noise factors [18]. Tables (6a-6c) and Figures (2a-2c) show the calculations of the mean of the (S/N) ratios for the three process variables with their different levels for weld bead characteristics.

**Table 6 (a): Mean of S/N ratios and rank for width according to OA L9 (3<sup>3</sup>)**

| Variable            | Variable levels  | (S/N) Ratio                   | Optimum level  | Delta=Max-Min | Rank |
|---------------------|--|-------------------------------|----------------|---------------|------|
| Welding current (I) | I <sub>1</sub> = 350<br>I <sub>2</sub> = 450<br>I <sub>3</sub> = 550 | 23.309-<br>25.537-<br>26.865- | I <sub>1</sub> | 3.556         | 1    |
| Arc voltage (V)     | V <sub>1</sub> = 26<br>V <sub>2</sub> = 27<br>V <sub>3</sub> = 28    | 24.832-<br>25.174-<br>25.706- | V <sub>1</sub> | 0.874         | 3    |
| Welding speed (S)   | S <sub>1</sub> = 400<br>S <sub>2</sub> = 500<br>S <sub>3</sub> = 600 | -26.319<br>25.585-<br>23.806- | S <sub>3</sub> | 2.513         | 2    |

**Table 6 (b): Mean of S/N ratios and rank for reinforcement according to OA L9 (3<sup>3</sup>)**

| Variable            | Variable levels  | (S/N) Ratio                 | Optimum level  | Delta=Max-Min | Rank |
|---------------------|--|-----------------------------|----------------|---------------|------|
| Welding current (I) | I <sub>1</sub> = 350<br>I <sub>2</sub> = 450<br>I <sub>3</sub> = 550 | 8-9.50<br>-8.620<br>-7.250- | I <sub>3</sub> | 2.258         | 2    |
| Arc voltage (V)     | V <sub>1</sub> = 26<br>V <sub>2</sub> = 27<br>V <sub>3</sub> = 28    | 30-9.9<br>618.7-<br>6.687-  | V <sub>3</sub> | 3.243         | 1    |
| Welding speed (S)   | S <sub>1</sub> = 400<br>S <sub>2</sub> = 500<br>S <sub>3</sub> = 600 | 9-9.53<br>98.54-<br>7.290-  | S <sub>3</sub> | 2.249         | 3    |



**Table 6 (c): Mean of S/N ratios and rank for penetration, according to OA L9 (3<sup>3</sup>)**

| Variable            | Variable levels      | (S/N) Ratio | Optimum level  | Delta = Max-Min | Rank |
|---------------------|----------------------|-------------|----------------|-----------------|------|
| Welding current (I) | I <sub>1</sub> = 350 | 13.980      | I <sub>3</sub> | 1.462           | 1    |
|                     | I <sub>2</sub> = 450 | 514.45      |                |                 |      |
|                     | I <sub>3</sub> = 550 | 215.44      |                |                 |      |
| Arc voltage (V)     | V <sub>1</sub> = 26  | 14.621      | V <sub>2</sub> | 0.500           | 3    |
|                     | V <sub>2</sub> = 27  | 14.878      |                |                 |      |
|                     | V <sub>3</sub> = 28  | 14.378      |                |                 |      |
| Welding speed (S)   | S <sub>1</sub> = 400 | 14.345      | S <sub>3</sub> | 0.610           | 2    |
|                     | S <sub>2</sub> = 500 | 614.57      |                |                 |      |
|                     | S <sub>3</sub> = 600 | 14.955      |                |                 |      |

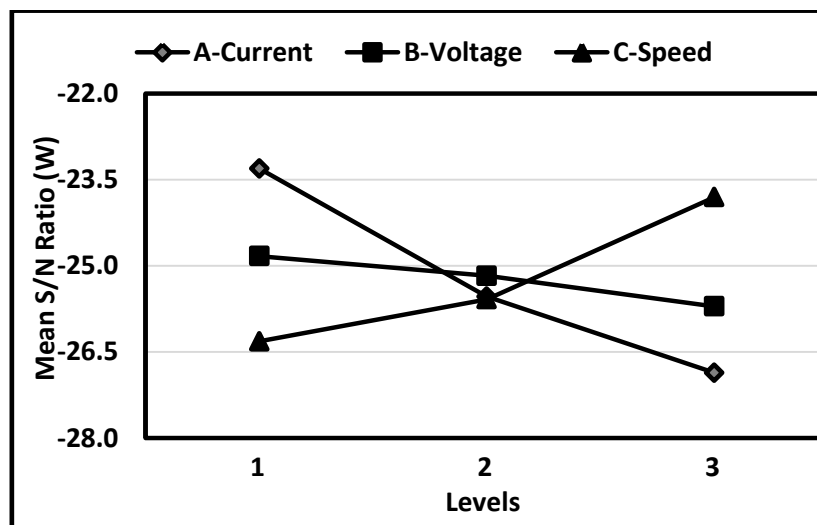


**Figure 2 (a): Effects of SAW variables on mean S/N ratios of (W)**

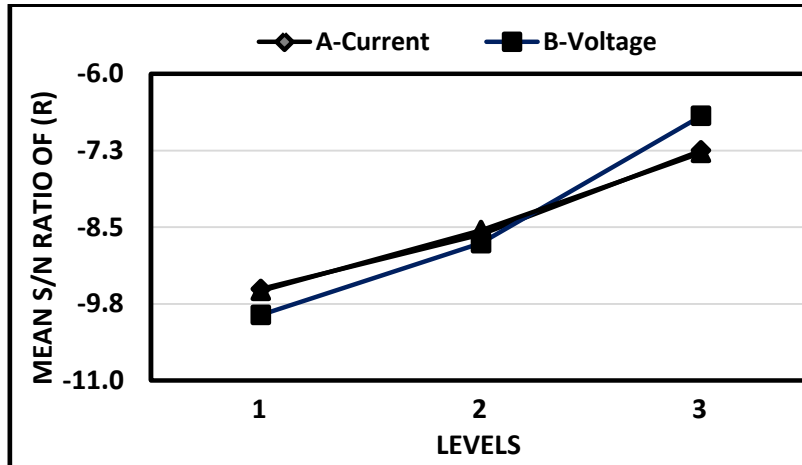


Figure 2 (b): Effects of SAW variables on mean S/N ratios of (R)

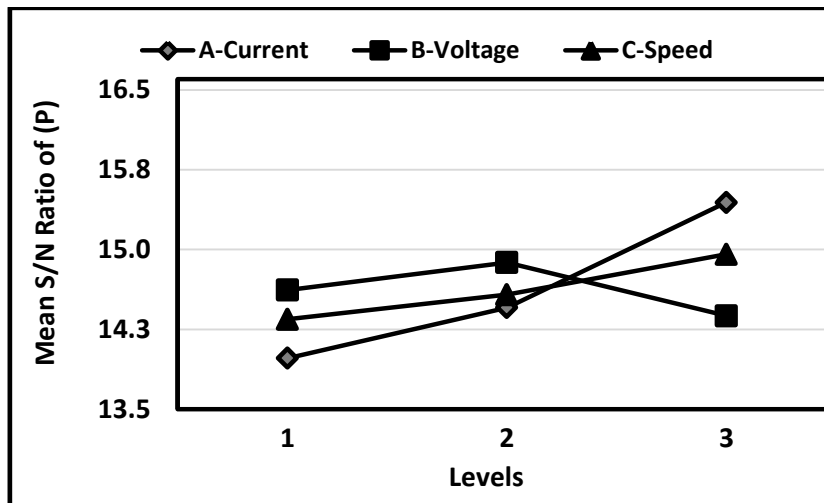


Figure 2 (c): Effects of variables on mean S/N ratios of (P)

**Analysis of Variance (ANOVA) According to OA L9 (3<sup>3</sup>):**

Tables (7a-7c) present the analysis of variance results for the signal-to-noise (S/N) ratios for the three performance characteristics.

**Table 7 (a): ANOVA results for (S/N) Ratio for width according to orthogonal array L9**

| Variable  | DF | SS      | Variance | F-Value  | p-Value | PeC     | Rank |
|-----------|----|---------|----------|----------|---------|---------|------|
| Current-A | 2  | 19.3726 | 9.6863   | 131.7721 | 0.0075  | 63.0934 | 1    |
| Voltage-C | 2  | 1.1633  | 0.5816   | 7.9125   | 0.1122  | 3.7885  | 3    |
| Speed-B   | 2  | 10.0218 | 5.0109   | 68.1680  | 0.0145  | 32.6393 | 2    |
| Error     | 2  | 0.1470  | 0.0735   |          |         | 0.4788  |      |
| Total     | 8  | 30.7046 |          |          |         | 100.000 |      |

**Table 7 (b): ANOVA results for reinforcement, according to orthogonal array L9 (3<sup>3</sup>)**

| Variable  | DOF | SS      | Variance | F-Value | p-Value | PeC     | Rank |
|-----------|-----|---------|----------|---------|---------|---------|------|
| Current-A | 2   | 7.7672  | 3.8836   | 7.6471  | 0.1157  | 23.7850 | 2    |
| Voltage-C | 2   | 16.2003 | 8.1002   | 15.9498 | 0.0590  | 49.6093 | 1    |
| Speed-B   | 2   | 7.6726  | 3.8363   | 7.5539  | 0.1169  | 23.4953 | 3    |
| Error     | 2   | 1.0157  | 0.5079   |         |         | 3.1103  |      |
| Total     | 8   | 32.6558 |          |         |         | 100.000 |      |

**Table 7 (c): ANOVA results for penetration, according to orthogonal array L9 (3<sup>3</sup>)**

| Variable  | DOF | SS     | Variance | F-Value  | p-Value | PeC     | Rank |
|-----------|-----|--------|----------|----------|---------|---------|------|
| Current-A | 2   | 3.3386 | 1.6693   | 187.1160 | 0.0053  | 77.5892 | 1    |
| Voltage-C | 2   | 0.3763 | 0.1882   | 21.0905  | 0.0453  | 8.7453  | 3    |
| Speed-B   | 2   | 0.5702 | 0.2851   | 31.9559  | 0.0303  | 13.2508 | 2    |
| Error     | 2   | 0.0178 | 0.0089   |          |         | 0.4147  |      |
| Total     | 8   | 4.3030 |          |          |         | 100.000 |      |

### 3.2 Discussion

The results from the analysis of the (S/N) ratios shown in Table 5 indicate that the optimum levels of the welding process variables are as follows: for the width is determined to be (I1V3S3) with the highest value of the (S/N) ratio is (-22.421) and the minimum (W) value achieved is (13.215mm) as in experiment No 3. However, for the reinforcement, the (S/N) ratio level is (I3V3S2), and the value of the (S/N) ratio is (-5.097), and the minimum (R) value is (1.800mm) as in experiment No 9. For bead penetration, the (S/N) ratio level is (I3V1S3) as in experiment no 7 with a value of (15.820) and the maximum (P) value is (6.180mm).

The outcome results from calculating the mean (S/N) ratio for each variable are presented in Table 6 and Figure 2. They revealed that the optimum levels of the welding process variables are as follows: for the weld bead width, the optimum level is (I1V1S3), whereas for the weld bead reinforcement, the optimum level is (I3V3S3), and for bead penetration is (I3V2S3).

After predicting the optimum conditions (levels) obtained from the mean (S/N) ratio for each variable, new confirmation experiments are designed and conducted with the new optimum levels of the welding variables. The purpose of these confirmation experiments is to validate the conclusions drawn during the mean (S/N) ratios analysis. The achieved optimum values for width, reinforcement, and penetration are 11.150mm, 1.4mm, 6.250mm, respectively.

By comparing the results of all variables for all output parameters using both the (S/N) ratios and the mean (S/N) ratios, the experimental results indicate the following: (a) any changes in the values of the design welding process variables can alter the performance characteristic. These variables play an essential role in the quality of welding operation [3][5]. (b) the experimental results also accentuate that the procedure of the mean (S/N) ratios calculations are better than

the procedure of (S/N) ratios analysis for determining the optimum level of the process variables [3][5].

The improvements in the bead parameters are as follows: (a) for the bead width is 15.6%, (b) for the bead reinforcement is 22.2%, and (c) for bead penetration is 1.1%.

According to the resulted mean (S/N) ratios and ANOVA analysis, as can be seen in Tables 6 & 7 and Figure 2, the effects of these are as follows:

**Bead Width:**

The welding current has the most significant effect on bead width followed by welding speed and, to less extent, the arc voltage. As the current increases, the width decreases, but as the speed increases, the width increases.

Welding current and speed are the main variables influencing the bead width, as shown in ANOVA analysis. The PeC of current, speed, and voltage on the bead width are 63.0934, 32.6393, and 3.7885, respectively. The p-values for both current (0.0075) and speed (0.0145) are less than 0.05, which is an indication that both variables are significant (current more critical than speed), where the p-value for the voltage is 0.1122. It is higher than 0.05 and indicates that voltage is an insignificant variable. Also, the F-value for the current and speed is higher than that of the voltage.

**Bead Reinforcement:**

The arc voltage significantly affects bead reinforcement than both current and speed, as shown in the mean (S/N) ratios and ANOVA results. From ANOVA analysis, voltage almost having a p-value equals 0.05. Still, both current and speed having p-values higher than 0.05 (0.1157) for current and (0.1169) for speed, so they have an insignificant effect compared to arc voltage.

The PeC of voltage, current, and speed on the bead reinforcement are 49.6093, 23.7850, and 23.4953, respectively. The F-value for the voltage is higher than both F-values for current and speed, and the higher, the more significant.

#### **Bead Penetration:**

All three variables influence the bead penetration with different rates, as shown in ANOVA analysis. Welding current is the most critical variable in determining the bead penetration, followed by speed and then voltage, as shown in the mean (S/N) ratios and ANOVA analysis results.

The bead penetration increases with the increase in the welding current. As the speed increases, the bead penetration increases, but the effect is less critical. The PeC of current, speed, and voltage on the bead penetration are 77.5892, 13.2508, and 8.7453, respectively. The p-values for all variables; current (0.0053), speed (0.0303), and arc voltage (0.0453) are less than 0.05. These values indicate that all these variables are significant (current more significant, followed by speed, and then voltage), where the F-values, the higher, the more significant the variable.

#### **4. Conclusion**

From the experimental results of this study, the following conclusions can be drawn:

1. The welding current is the primary variable that significantly influences the bead width and penetration, followed by welding speed and then the arc voltage. The arc voltage is the most crucial parameter in determining the bead reinforcement, followed by current and then speed.
2. The optimum levels of the process variables are as follows: (a) for the width are ( $I_1 V_1 S_3$ ) (350A, 26V, 600mm/min), (b) for the

reinforcement are ( $I_3V_3S_3$ ) (550A,28V,600mm/min), and (c) for the penetration are ( $I_3V_2S_3$ ) (550A,27V,600mm/min).

3. The improvements in the bead parameters are: (a) for the bead width is 15.6%, (b) for the bead reinforcement is 22.2%, and (c) for bead penetration is 1.1%.
4. The PeC of welding current, welding speed, and arc voltage on the bead width are 63.0934, 32.6393, and 3.7885, respectively. The F-value for current is (131.7721), for speed is (68.1680), and for voltage is (7.9125); this is a strong proof that both the current and speed are the most important variables influencing the bead width and that the current is more significant than speed.
5. The PeC of arc voltage, welding current, and welding speed on the reinforcement are 49.6093, 23.7850, and 23.4953, respectively. The F-value for voltage is (15.9498), for current is (7.6471), and for speed is (7.5539), which indicates that voltage influences bead reinforcement more than current and speed.
6. The PeC of welding current, welding speed, and arc voltage on the penetration are 77.5892, 13.2508, and 8.7453, respectively. The F-value for current is (187.1160), for speed is (31.9559), and for voltage (21.0905); this is a strong proof that the current is the most critical variable influencing the bead penetration.


## References

- [1] Houldcroft, P. (1989), "Submerged-arc welding", Woodhead Publishing Limited, Cambridge, UK, 2<sup>nd</sup> Edition.
- [2] Singh, R. (2020), "Applied welding engineering processes, codes, and standards", 3<sup>rd</sup> Edition, Butterworth-Heinemann, Elsevier Inc.
- [3] Akbar, A. and Kadhim, H. (2015), "Prediction of bead width in submerged arc welding of low carbon steel (AISI 1005)", Engineering and Technology Journal, 33(2), pp. 451-460.
- [4] Al-Dawood, Z. and Saadon, A. (2015), "Optimization process variables of submerged arc welding using the Taguchi method", International Journal of Engineering and Advanced Technology (IJEAT), 5(1), pp. 149-152.
- [5] Karaoglu, S. and Secgin, A. (2008), "Sensitivity analysis of submerged arc welding process parameters", Journal of Material Processing Technology, 202, pp. 500-507.
- [6] Jain, A., Bansal, P., and Khanna, P. (2018), "Development of mathematical models to analyze and predict the weld bead geometry in submerged arc welding of low carbon alloy steel", International Journal on Emerging Trends in Mechanical & Production Engineering, 2(1), pp. 1-8.
- [7] Choudhary, A., Kumar, M., and Unune, D. (2018), "Experimental investigation and optimization of weld bead characteristics during submerged arc welding of AISI 1023 steel", Defence Technology, 15(1), pp. 72-82.
- [8] Vedrtnam, V., Singh, G., and Kumar, A. (2018), "Optimizing submerged arc welding using response surface methodology, regression analysis, and genetic algorithm", Defence Technology, 14(3), pp. 204-212.
- [9] Abohusina, A. (2018), "Determining the optimum welding parameters on the weldability of mild steel using submerged arc welding process", MSc, Department of Mechanical



- Engineering and Energies, School of Engineering and Applied Sciences, Libyan Academy for Postgraduate Studies, Janzur, Libya.
- [10] Al-Dawood, Z. and Saadoon, A. (2017), “Multi response Optimization of submerged arc welding using the Taguchi fuzzy logiv based on utility theory”, *International Journal of Science and Research (IJSR)*, 6(12), pp. 475-481.
- [11] Pu, J., Yu, S. and Li, Y. (2017), “Parameter optimization of flux-aided backing-submerged arc welding by using the Taguchi method”, *International Journal of Modern Physics B*, 31, pp. 16-19.
- [12] Deshmukh, P. and Teli, S. (2014), “Parametric optimization of SAW welding parameters using Taguchi L9 Array”, *International Association of Scientific Innovation and Research*, 8, pp. 43-47.
- [13] Sharma, M. and Khan, M. (2013), “Optimization of SAW process parameters for bead geometry of bead-on-plate welds deposited on structural steel IS-2062 using Taguchi method”, *International Journal of Science and Research*, 4(3), pp. 2322-2325.
- [14] Bhardwaj, S. et al. (2015), “Optimization of weld bead geometry in submerged arc welds deposited on En24 steel alloy using Taguchi method”, *Journal of Mechanical and Civil Engineering*, 12(6), pp. 18-21.
- [15] Datta, S., Bandyopadhyay, A. and Kumar, P. (2008), “Grey Based Taguchi method for optimization of bead geometry in submerged arc bead-on-plate welding”, *International Journal of Advanced Manufacturing Technology*, 8, pp. 1136-1143.
- [16] Barma, J. et al. (2012), “Process parametric optimization of submerged arc welding by using utility-based Taguchi concept”, *Advanced Materials Research*, 488, pp. 1194-1198.
- [17] Frefer, A. and Abohusina, A. (2021), “The effect of the submerged arc welding variables on bead geometry of mild

- steel using regression analysis technique”, Journal of Engineering Research, March 2021, pp. 35-50.
- [18] Kumanan, S., Edwin, J. and Gowthaman, K. (2007), “Determination of submerged arc welding process parameters using Taguchi method and Regression analysis”, Indian Journal of Engineering & Material Sciences, 14, pp. 177-183.
- [19] Ross, P. (1988), “Taguchi techniques for quality engineering”, McGraw-Hill, New York.
- [20] Hatab, A. and Zaid, H. (2008), “Optimizing cutting parameters for surface roughness in turning of the commercial aluminium (1100-H18 type) alloy using Taguchi method”, 40<sup>th</sup> International Conference on Mining and Metallurgy, Sokbanja, Serbia, pp. 515-524.



**Behavioral Intention of Youth Using  
Facebook in Learning in Libya (Bani  
Waleed as Model)**

**6**



## Behavioral Intention of Youth Using Facebook in Learning in Libya (Bani Waleed as Model)

Imman Ahmed Mohammed

Computer Department, Faculty of Science, Bani Walid University

[red.mana@yahoo.com](mailto:red.mana@yahoo.com)

Abdulkarim Saleh Masoud Ali

Automation Department, Harouge Oil Operations

[Abdulkarimali84@gmail.com](mailto:Abdulkarimali84@gmail.com)

Haitham S. Ben Abdelmula

Libyan Center for Electronic Systems, Programming and Aviation Research

[hsaa8383@gmail.com](mailto:hsaa8383@gmail.com)

Hend Abdelgader Eissa

Electronic Technology College

[haseissa@icloud.com](mailto:haseissa@icloud.com)

Wan Rozaini Bt Sheik Osman

School of Computer, University Utara Malaysia

[Rozai174@uum.edu.my](mailto:Rozai174@uum.edu.my)

### **Abstract**

Social media is becoming increasingly important in many lives, especially youths. However, many people are not able to get access and for those who do, may not use it positively. The present study intends to investigate the perceptions of youths in the city of Bani waleed, Libya, towards the use of Facebook in learning. The investigation was based on the Technology Acceptance Model (TAM). Variables from model were tested using a quantitative

approach with a set of questionnaires which was distributed among 350 youths from 2 high schools in the city of Bani waleed, Libya. The unit of analysis consists of 119 males and 97 females aged between 16 to 23 years old. The findings from the study highlighted the perceptions and acceptance of the use of social media among youths in the selected population, where the main purpose was for entertainment and education. Others used Facebook for maintaining relationship with family and friends as well as find new friends.

**Keywords:** social media – facebook - technology acceptance model (TAM)- social media acceptance in learning.

## **1. Introduction**

Social media are becoming very important media nowadays in terms of communication and information and people are possessed to it. The media is used for multiple purposes by different religion and race globally, for private, business, public and academic undertakings. Social media is used for social and business interaction and also support teaching students in the classroom, as source of vast knowledge and information are available in split of seconds [1][2].

Social media is a set of complex tools that can be utilized to involve the youth's knowledge and thinking maturity. Social media has both positive and negative impact and implementation on the youth if it is not managed and controlled appropriately, may lead to negative influence. However, the evolution of social media potentially has a larger influence than that, in which, has impact on youth as a double edge sword. It has influenced many people globally, including people of Libya. "These influences of social media, which has enhanced the exposure of the people to technology, have created more awareness among youth. Youth is highly involved in social media" [3].

## **2. Problem Statement**

Previous studies have shown the effect of social media in the positive aspect in education. Yet, many youths are exposed not only to physical danger, but as well as online threats from the people or known as the negative aspect of social media [1]. However, it is significant to look at the positive properties of social media, especially Facebook (FB), this study focuses on using Facebook, because Facebook is most used in Libya. to be able to give a clear image of what the benefits and threats of using social network sites are. The youths face different challenges and will choose to do different things on FB. There is currently limited research on how Libyan youths use FB, and this study will attempt to obtain empirical data to identify the current use, and intention to use that will provide input for schools, and parents to maximize the youth use of FB. Furthermore, proper planning and awareness programmers can be designed to help the youth gain benefits from using FB [1].

This research examines the youth's usage of Facebook in learning context that influence their attitude, perceived usefulness, perceived ease of use and social norm.

## **3. Research Questions**

The research question is as follows;

- i. What is the behavioural intention of using Facebook among youths in Libya?
- ii. What factors influences youths to use Facebook in Libya?
- iii. How do the youth use Facebook?

## **4. Research Objectives**

The objectives of this research are:

- 1) To determine the behavioural intention in using Facebook among the youth in Libya.

- 2) To identify the factors that can influence the use of Facebook among youths in Libya.
- 3) To investigate how youth use Facebook in Libya.

## **5. Literature Review**

Social network is an interaction tool used by group of people, to enable them to communicate on both private and academic life matters [1]. It is done through a network that communicates with the group of users, text messages, audio and video display and imaging picture in full color high definition. By late 2010, there are approximately 2 billion users of internet and approximately 45 million users alone in the Arab world. According to [4], there are more than 135 million individuals using the Internet in the 22 Arab countries. This is coupled with a mobile penetration rate of around 110 percent on a regional level; and more than 71 million active users of social networking technologies. With the huge potentials and advancements, and high demand element, youth using SNS is going to strengthen the new communication technology era, which will benefit the Arab World, in long information, business and personal oriented relationship global instant news updates.

Youth is commonly defined as the time of life between childhood and adulthood (maturity). Definitions for the specific age for youth collection vary. Usually, it refers to the public legal age that is below the age of 23 years. Youth is a term used for people of both genders, male and female, of young age [5].

In this paper, Facebook social networking application is used as an important tool in higher education learning as the benefits on the learners [1]. According to a study in Libya by [6], it was found that 93.4% of the users had heard about Facebook. So based on previous research, this study will focus on Facebook as a tool for learning which is mostly used in Libya.



Wadie and Lanouar study examine the Technology Acceptance Model (TAM) within the context of Facebook and confirms that this model is useful to explain Facebook adoption. There are many constructs compiled into the structural model to explain factor of the adoption of Facebook, i.e. information receiving, self-efficacy, perceived usefulness, perceived ease of use, social norm, attitude and adoption to use Facebook [7]. Figure 1, shows the TAM model with its fundamental elements.

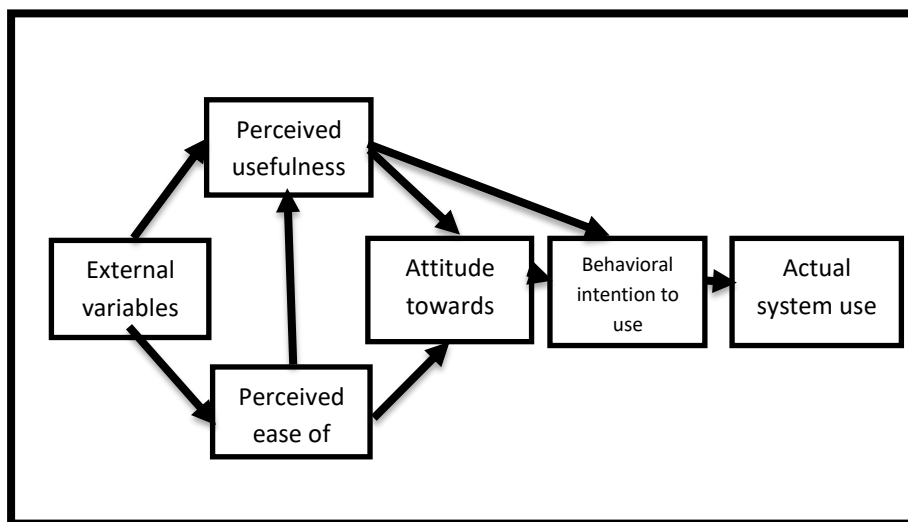


**Figure 1: Technology Acceptance Model (TAM) [7]**

Davis and others suggested the TAM is used to determine the consumer's actual acceptance of the IT. TAM shall be used to analyses and increase the acceptance. Moreover, it is achieved through consumer's action (explanation) across various computing technology with the assumption that actual technology users are determined by Behavioural Intention (BI) [8].

This had direct positive correlation over the effect of the attitude. For example, [9] exposed that the relationship was significant perceived ease of use and perceived usefulness. Therefore, based on the

theoretical and empirical support from the information technology literature, this study proposes a conceptual model”.

## **6. METHODOLOGY**

This study is a quantitative study, focusing on a particular sample of the selected population. Previous studies have been found to be scarce in the investigated area of the study, thus the need to fill in the gap. This study will capture a snapshot view of the current behavioral intention of the respondents, mainly in the adoption of a social media application, namely Facebook, as a social networking tool that may have an impact on learning among the youths in Libya.

In previous studies, researchers have stressed that high school students have shown interest in using tools supported learning activities, especially during interactions, collaboration, active participation, information and resource sharing.

In Libya, schooling youths are found to be deeply engaged in the use of Facebook and other kinds of networking tools. The objective of the present study is to determine the relationship of high school students' intention to use Facebook in 2 selected schools in the city of Bani waleed. The framework of the present study is adapted from the TAM model within selected constructs; such as their attitudes, perceived usefulness, and perceived ease of use, and social norm.

A questionnaire was designed to capture the youth's opinion and awareness of using social media. The collected data from the participants was then analyzed using Statistical Package for the Social Sciences (SPSS) [1].

The sampling population for this study is selected based on the fact that the students from schools in Bani waleed have the same level of education background, thus contributing to homogeneity of the data gathered, which is important to control the homogeneity of the data in order to avoid any issues related to generalizability of the findings. In social science research, unit of analysis is defined as the major entity that is being analyzed. For the present study, data collected in the form

of the perception of individual youths from schools in Bani waleed. The units of analysis were selected among youths aged between 16 to 21 years old. From the selected population, 119 males and 97 females were chosen and given the questionnaire.

A random sampling approach which applied to the selection of the students from these 2 schools to be given the set of questionnaires to eliminates the possibility of gathering biased samples [10]. In this study 350 questionnaires have been sufficient and distributed in 2 schools with total students almost 10.000 in accordance with the sample size.

Figure 2 shows the flow of the research which started with Stage 1, that is gaining access to the selected population and the selection of participants for the study. The questionnaire was adapted from the literature and validated by an academic expert in the Bani Waleed University. A pilot study was carried out with 30 students from the samples taken from the population to test the reliability of the questionnaire. In order to measure the accuracy of the findings, the responses from the questionnaire during the pilot study were examined using the statistical Cronbach's alpha test. The next stage was the data collection stage. The questionnaire is distributed to the selected samples. Here, the participants were required to respond to the given set of questionnaires, followed by the gathering of the questionnaires. The final stage was the data analyzed and tabulated, to find the answers for the research questions. The three stages of the study were taken in order to complete the investigation of the perceptions of the students from the 2 selected schools, in terms of using Facebook as a tool for learning activities. Once this was achieved, the research questions were answered accordingly.

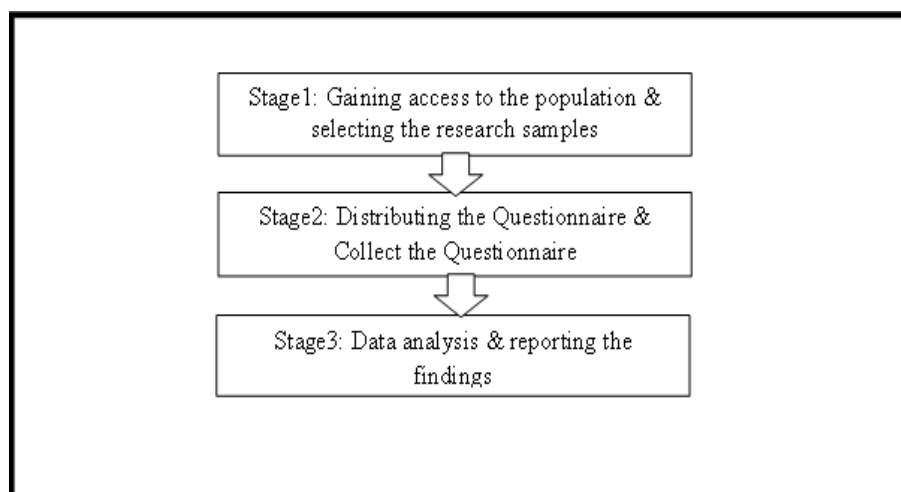


**Figure 2: The Research Procedures**

Issues related to validity and reliability was addressed by controlling the variables involved such as the level of education background of the participants and the locations of the schools. However, as random sampling method is applied to the selection of the participants, the issue of gender equality might cause some sort of limitation to the study.

## **7. RESULTS AND DATA ANALYSIS**

Data were collected from two high schools in Libya. From the selected schools, 300 students had participated to answer the questionnaire related to the behavioural intention of youth in using Facebook. After the collected data was analyzed, it was found that 84 students did not completely answer the questionnaire. Subsequently, the remaining 216 questionnaires were used and were accounted for the data analysis.

The population size of this study is composed of 10000 students studying in high school Sana Muhidale and Seventh of April. The table computed the value of 350 as a suitable sample size [11]. Therefore, this study distributed 300 questionnaires as link to students

through Facebook. An unbiased sample is very important to get accurate results and simple random sampling provides unbiased response.

### 10.1 Response Rate

According to [11], 30 percent response rate could be enough in case of surveys. Thus, the response rate of this study is considered adequate and acceptable. Table (1) shows the number of questionnaires distributed, the number of completely filled questionnaires returned, and the response rate (in percentage) of the survey questionnaires received.

**Table - 1: Response by Rate of the Survey**

| Response                             | Frequency/ Rate |
|--------------------------------------|-----------------|
| Number of distributed questionnaires | 350             |
| Returned Questionnaires              | 300             |
| Response Rate                        | 85.7%           |
| Completed questionnaires             | 216             |

### 10.2 Demographic Information

Demographic profile contains of four different sections; gender of the respondents, age of the respondents, their year of study and the school in which they are enrolled as shown in Tables 2, 3, 4 and 5.

**Table - 2: Gender**

| Gender | Frequency | Percent |
|--------|-----------|---------|
| Male   | 119       | 55.1    |
| Female | 97        | 44.9    |
| Total  | 216       | 100.0   |

**Table - 3: Age**

| <b>Age</b> | <b>Frequency</b> | <b>Percent</b> |
|------------|------------------|----------------|
| 15-17      | 49               | 22.7           |
| 18-20      | 77               | 35.6           |
| 21-23      | 90               | 41.7           |
| Total      | 216              | 100.0          |

**Table - 4: School**

| <b>School</b>    | <b>Frequency</b> | <b>Percent</b> |
|------------------|------------------|----------------|
| Seventh of April | 117              | 54.2           |
| Sana Muhidale    | 99               | 45.8           |
| Total            | 216              | 100.0          |

**Table - 5: Years**

| <b>Year</b> | <b>Frequency</b> | <b>Percent</b> |
|-------------|------------------|----------------|
| 1           | 49               | 22.7           |
| 2           | 52               | 24.1           |
| 3           | 58               | 26.9           |
| 4           | 57               | 26.4           |
| Total       | 216              | 100.0          |

The older age of the respondents may influence their ability to the adoption of the technology, while the younger students may show opposite ability to adapt to new technologies in learning. This may also be the case when it comes to understanding technology-based

instructions, where technical terms are frequently used and reflected in the integration of technology into learning instructions. Parents' control over the younger group of respondents may also indicate a lower response to the use of social media such as Facebook.

The highest number of respondents from the third year of study shows that the responses were given by those who are equipped with some knowledge of higher learning and are ready for the integration of social media into learning. This is also supported by indication of the second highest number of respondents from the fourth year of study, as indicated in the table.

### 10.3 The Purpose of Using FACEBOOK

Table 6 presents the purpose of using Facebook. The respondents indicated that most of the time, they use Facebook for the purpose of Entertainment and Education. The high indication for Entertainment and Education shows that most of the respondents prefer to use Facebook for entertainment and also for education via social media.

The respondents seem to prefer integrating education with entertainment when learning via Facebook, rather than to learn alone. It is found that there are certain websites that have started promoting their online learning programs through Facebook.

**Table - 6: The purpose of using the Facebook**

| Purpose                  | Frequency | Percent |
|--------------------------|-----------|---------|
| Entertainment            | 10        | 4.6     |
| For the new in all areas | 14        | 6.5     |
| To connect with friends  | 9         | 4.2     |
| Education and friendship | 8         | 3.7     |
| Education                | 15        | 6.9     |
| Follow the news          | 6         | 2.8     |

|  |            |              |
|--|------------|--------------|
| Entertainment and education              | 31         | 14.4         |
| The friendship                           | 22         | 10.2         |
| Education and surveys                    | 9          | 4.2          |
| For conversation and replace information | 15         | 6.9          |
| For all the news                         | 1          | 0.5          |
| Viewing                                  | 11         | 5.1          |
| know the news around the world           | 4          | 1.9          |
| Follow the news                          | 10         | 4.6          |
| long relationship                        | 26         | 12.0         |
| Learn                                    | 4          | 1.9          |
| Conversation                             | 13         | 6.0          |
| The culture                              | 8          | 3.7          |
| <b>Total</b>                             | <b>216</b> | <b>100.0</b> |

Table 7 shows the duration that respondents spend for using Facebook per day.

**Table - 7: Time spent using Facebook (per day)**

| Facebook per day  | Frequency  | Percent      |
|-------------------|------------|--------------|
| Never             | 6          | 2.8          |
| 1-2 hours         | 66         | 30.6         |
| 3-4 hours         | 67         | 31.0         |
| More than 4 hours | 77         | 35.6         |
| <b>Total</b>      | <b>216</b> | <b>100.0</b> |



#### 10.4 Reliability

Reliability assessment was conducted on Perceived ease of use, Perceived usefulness, Attitude, Behavioural intention and Social/Subjective norm. The Cronbach's alpha values of the variables tested in the study are shown in Table 8. Table 8 also shows the Cronbach's alpha test to determine the internal consistency and reliability for the five variables. The commonly used value for Cronbach's alpha is 0.70 for the lower limit of acceptability. Values more than 0.7 indicate that the items for each variable are homogeneous and measuring the same constant. Thus, the Cronbach's alpha values for the tested variables are in the accepted and consistent range.

**Table - 8: Reliability**

| Variable               | Item | A     |
|------------------------|------|-------|
| Perceived ease of use  | 7    | 0.76  |
| Perceived usefulness   | 6    | 0.846 |
| Attitude               | 7    | 0.858 |
| Behavioural intention  | 3    | 0.765 |
| Social/Subjective norm | 7    | 0.921 |

#### 10.5 Evaluation

Descriptive statistical analysis was conducted in order to provide an in-depth understanding of the relationship among the variables of the study. Subsequently, descriptive statistical analysis is used to explain the construct of the items in the questionnaire. In this paper, the detailed analysis is interpreted according to individual variables that were tested, namely: Perceived ease of use, Perceived usefulness, Attitude, Behavioural intention and Social/Subjective norm. Table 9 shows the analysis in the form of mean and standard deviation.

**Table - 9: Mean and Standard Deviation**

| <b>Variable</b>        | <b>Minimum</b> | <b>Maximum</b> | <b>Mean</b> | <b>Standard Deviation</b> |
|------------------------|----------------|----------------|-------------|---------------------------|
| Perceived ease of use  | 1.00           | 5.00           | 4.0437      | 1.06904                   |
| Perceived usefulness   | 1.00           | 5.00           | 4.1049      | 1.13315                   |
| Attitude               | 1.00           | 5.00           | 4.1409      | 0.89161                   |
| Behavioural intention  | 1.00           | 5.00           | 3.6836      | 1.21073                   |
| Social/Subjective norm | 1.00           | 5.00           | 4.1052      | 0.93042                   |

Perceived usefulness shows that the respondents perceived well to the use of Facebook, indicating that it is easy to use Facebook compared to other social media sites. According to the analysis, perceived usefulness is second item that affected the use of Facebook among students in Libya.

The mean value for Attitude is 4.1409 while the standard deviation is 0.89161. This indicated that the respondents' attitude towards the use of Facebook is highly positive and supportive. Almost all of the respondents indicated that they are happy with Facebook and confirming the positivity by indicating a near 5 values of mean.

Significantly, this indicates that the respondents are keen on social interaction and has made it a norm of life when it comes to corresponding with friends and family, using the Facebook. This also shows that the respondents are highlighting the use of Facebook for entertainment purposes and maintaining long term relationships, as indicated in the Purpose of using Facebook section of the questionnaire.

## **8. CONCLUSION**

This study was conducted with the aim to investigate the perceptions of youths in the city of Bani waleed, Libya, towards the use of Facebook. The investigation was based on the Technology Acceptance Model (TAM). Five variables, namely; Perceived ease of use, perceived usefulness, Attitude, Behavioural intention and Social/Subjective norm, were tested towards the use of Facebook.

The research instrument used for this particular study consists of a set of questionnaires designed by adapting various elements from previous studies from the literature. In order to validate and provide constant evidence, the data gathered was analyzed using various statistical analyses methods including the data screening, descriptive statistical data analysis, regression analysis and reliability analysis.

From the data analysis, it was found that majority of the respondents are using Facebook as frequently as more than four hours a day. Most of the respondents also agreed that they use Facebook from 3 to 4 hours a day. On the contrary, only 6 respondents stated that they have never used Facebook at all.

All the selected respondents were found to be actively using Facebook for various different reasons from Entertainment and Education, to maintaining Long Relationship, for the purpose of Friendship to Conversation and Replace Information, Know the News around the World and to Learn.

## References

- [1] Al-Mukhaini, E. M., Al-Qayoudhi, W. S., & Al-Badi, A. H. (2014). Adoption of social networking in education: A study of the use of social networks by higher education students in Oman. *Journal of International Education Research (JIER)*, 10(2), 143-154.
- [2] Ghannam, J. (2011). *Social Media in the Arab World: Leading up to the Uprisings of 2011*. Center for international media assistance, 3. Al-Mukhaini, E. M., Al-Qayoudhi, W. S., & Al-Badi, A. H. (2014). Adoption of social networking in education: A study of the use of social networks by higher education students in Oman. *Journal of International Education Research (JIER)*, 10(2), 143-154.
- [3] Boyd, D. (2007). Social Network Sites: Definition, History, and Scholarship. *Computer Mediated Communication*, 3-20.
- [4] Jamali, R. (2014). *Online Arab Spring: Social media and fundamental change*. Chandos Publishing.
- [5] Rantai, A., Hamdan, M. D., & Hamid, S. S. A. (2014). Influence of Social Media in Enhancing Positive Relationship among Youth. In the proceedings of Seminar Kebangsaan Integriti Keluarga 2014. University Malaysia Sabah.
- [6] Sekaran, U., & Bougie, R. (2011). *Research Methods for Business: A Skill Building Approach (5th ed.)*: WILEY.
- [7] Wadie, and Lanouar Charfeddine. "Factors affecting the adoption of Internet banking in Tunisia: An integration theory of acceptance model and theory of planned behavior." *The Journal of High Technology Management Research* 23, no. 1 (2012): 1-14.
- [8] Davis, F. D., Bagozzi, R. P., & Warshaw, P. R. (1989). User acceptance of computer technology: A comparison of two theoretical models. *Management Science*, 35(8), 982-1003.

- [9] Moon, J. & Kim, Y. (2001). Extending the TAM for a World-Wide-Web context. *Information and Management*, 38, 217-230.
- [10] Borden, KS & Abbott, BB (2008). *Research Design and Methods: A Process Approach*. (7 Edition). New York: McGraw Hill.
- [11] Sekaran, U., & Bougie, R. (2003). *Business Research Methods*.